Evolution-Development Congruence in Pattern Formation Dynamics: Bifurcations in Gene Expressions and Regulation of Networks Structures

Takahiro Kohsokabe[1], Kunihiko Kaneko[1,*],

1 Department of Basic Science, Graduate School of Arts and Sciences, The University of Tokyo, 3-8-1 Komaba, Meguro, Tokyo, Japan

∗ **E-mail: kaneko@complex.c.u-tokyo.ac.jp**

arXiv:1402.5214v1 [q-bio.PE] 21 Feb 2014

Abstract

Deciphering and understanding potential relationships between evolution and development has been an important research goal for over a century. Recent advancements in quantitative analyses based on comparative genomics and massive gene expression data suggest that the time is ripe to uncover new relationships on phylogeny and ontogeny. By representing the developmental dynamics of spatially located cells with gene expression dynamics involving cell-to-cell interactions, under an external morphogenic gradient, we numerically evolved gene regulation networks, subject to mutation and selection, as they approach a prescribed spatial pattern of expressed genes. From analyses of hundreds of numerical evolution experiments, remarkable congruence was observed between generational change in patterns through evolution along a single chain phylogeny and that through developmental process of the evolved descendant. Here, both of the pattern dynamics consisted of several epochs capable of producing successive stripe formations between quasi-stationary regimes. These epochs are represented as bifurcations in dynamical-systems theory, and thus the evolution-development congruence is understood as a correspondence of bifurcation. A quasi-stationary regime in development is due to component(s) with slowly varying expression, while in evolution, generations are needed to produce relevant mutations. The evolved developmental dynamics are regulated by successive combinations of feedback or feedforward regulation under the upstream feedforward network to read the morphogen gradient. A novel pattern-formation mechanism was also uncovered, in which temporal oscillation by a feedback loop is fixed to a spatial stripe by cell-to-cell interaction under a boundary set by the upstream feedforward network. We report an exceptional violation to the evolution-development congruence, which originated from alteration of the boundary due to mutation in the upstream feedforward network. Our results provide a new look on possible parallelism between evolution and development, existence of developmental stages, punctuated equilibrium, developmental bottlenecks, and evolutionary acquisition of novelty in morphogenesis.

Author Summary

Although the phrase “ontogeny recapitulates phylogeny” turned out to be incorrect, the search for possible relationships between development and evolution still gathers much attention. Recently, dynamical-systems analysis has proven to be relevant to both development and evolution, and it may therefore provide a link between the two. Using extensive simulations to evolve gene regulation networks that shape morphogenesis, we observed remarkable congruence between development and evolution: Both consisted of the same successive epochs to shape stripes, and good agreement was observed for the ordering as well as the topology of branching of stripes between the two. This congruence is explained by the agreement of bifurcations in dynamical-systems theory between evolution and development, where slowly varying gene-expression levels work as emergent control parameters. In terms of the gene regulation networks, this congruence is understood as the successive addition of downstream modules, either as feedforward or feedback, while the upstream feedforward network shapes the boundary condition for the downstream dynamics, based on the maternal morphogen gradient. Acquisition of a novel developmental mode was due to mutational change in the upstream network to alter the boundary condition. Our results provide

a fresh perspective on evolution-development relationship, as well as on the acquisition of developmental novelty.

Introduction

The possible relationships between the development of multicellular organisms and their evolution have been the subject of intense research over a century. About 200 years ago, von Baer proposed laws of development, based on observations of development across species, which mainly claimed that the early embryo is mostly conserved across species, while embryonic changes through ontogeny move from a general form common to many species, to species-specific forms [1]. Charles Darwin and other biologists of his time interpreted these laws as proof of evolution from a common ancestor [2–4]. Thus, changes in embryos from a common to a specialized form are regarded as a reflection of evolutional history. Development has been studied in an evolutionary context, and so many biologists have searched for possible relationships between evolution and development. While Ernst Haeckel's claim that 'Ontology recapitulates phylogeny' have been proved incorrect, the search for potential relationships between development and evolution has continued to be of interest to many biologists [5–7].

Previously, this type of research was hindered by a lack of quantitative arguments. To transcend the century-long controversies associated with this research, efforts are being made to quantitatively analyze the evolution-development ('evo-devo') relationship by using gene expression and genome sequence data. In particular, an hourglass hypothesis has been proposed related to the existence of a developmental bottleneck, where differences in gene expressions among several species from the same progenitor decreases at the same developmental stage. This hypothesis suggests that there is a species-wide common stage in development where embryos of different species are similar both in morphology and gene expression patterns [8–14]. In spite of these advances, however, a general relationship between evolution and development, as well as its origin, if it exists, remains to be unveiled owing to the limitations in available data on developmental processes along the evolutionary course.

Species-wide comparison is made using phylogenic trees with branchings to different species, as schematically shown in Fig.1. On the other hand, one can compare a comparison over species along a single phylogenetic chain from ancestor to offspring. Ontologies are compared across ancestors along a single evolutionary chain, as shown in Fig. 1. This comparison is rather difficult in practice, as fossil data usually do not include information on developmental processes. However, such comparison, if available, gives more straightforward information on relationship between development and evolution, and will provide a basis for species-wide comparison. With such single-chain comparisons, one can gain insight of possible mechanisms that may give evo-devo relationship.

In contrast to experimental difficulty, however, such single-chain comparison is available by taking advantage of in-silico evolution. Indeed, several numerical evolution of developmental process has been recently carried out, by using dynamical-systems models. These models consider the spatial arrangements and behaviors of cells that are subject to morphogenic gradients and cell-to-cell interactions, and simultaneously project protein expression level changes within the cells over time by intra-cellular gene expression dynamics. The developmental processes of cellular states are represented by these gene expression dynamics with cell-to-cell interactions to form a spatial pattern of expressions, while the evolution of the gene regulation networks associated with these dynamics are modified by genome changes. By establishing a fitness condition to select a specific pattern, the evolution of the network to generate such a pattern can be studied quantitatively. Indeed, with this setup, recent studies of in silico evolution have suggested basic mechanisms for stripe formation through development. By establishing conditions to form some number of stripes, two basic modes of gene expression dynamics are revealed, which are generated as a result of feedforward and feedback gene-regulation networks [15–18, 20]. These unveiled mechanisms correspond to the two developmental modes in arthropods, i.e., long-term and short-term development, while the detected basic structures in gene regulation networks show some correspondence with those

observed in several organisms. So far, however, the relationship between developmental processes across individuals along an evolutionary course has not been explored.

Following former theoretical studies for stripe formation, we focus here on uncovering evo-devo relationship by introducing a fitness condition so that the gene-expression of a given output gene in space approaches a prescribed spatial pattern which is not necessarily periodic in space. Comparing the developmental processes to shape a given gene-expression pattern through an evolutionary course under mutation, we found parallelism between evolution and development along the single-chain phylogeny. We name this parallelism as evo-devo congruence, which is observed for the majority of simulation instances. This congruence is based on the correspondence of epochs. In fact, both development and evolution consist of a few epochs that rapidly change to form new stripes, and the slow quasi-stationary regimes between two epochs. Here, drastic change in patterns at each epoch is understood in terms of bifurcation in dynamical systems theory. Both development and evolution adopt the same type of bifurcation to generate epochs that are parallel between evolution and development. Gene regulation networks used to achieve such developmental dynamics are found to consist of a combination of an upstream feedforward network with downstream feedforward or feedback networks. The upstream feedforward network can provide the boundary conditions of same expression levels, through which the temporal oscillation by the downstream feedback network is embedded into a spatial stripe pattern. In rare examples, however, evo-devo correspondence is found to be violated, where change in the upstream feedforward network alters the downstream stripe formation. After first examining extensive numerical results to support the above conclusion, its relevance to biological development and evolution will be discussed.

Results

We numerically evolved gene regulatory networks governing development in order to study evo-devo relationship. Here each organism consisted of $M(= 96)$ cells aligned in one-dimensional space, where maternal factors were supplied from each end of the space. Each cell had $N(= 16)$ genes (proteins) whose expression dynamics were governed by expression levels of other genes through a given gene regulatory network (GRN), while interaction between neighboring cells was mediated via diffusion of expressed proteins. These conditions defined the developmental dynamics of the study. We prepared 100 individuals with slightly modified GRNs. After each gene expression level reached a stationary value through development, we computed fitness from the expression of a prescribed target gene.

Fitness was defined as the difference between this output expression pattern in space and a prescribed target pattern, with the highest fitness values defined by the best match. We used a genetic algorithm to select the individuals with higher fitness by introducing mutations in the GRN (See Fig. 2 for schematic representation and Methods for details).

Most evolved networks, after few thousand generations, were capable of generating predefined target patterns. An example of the developmental time course to shape such a pattern is given in Fig. 3A, where the space-time diagram of the expression level of the output gene is displayed with the horizontal axis as the developmental time and the vertical axis as the cellular index (i.e., spatial axis). As shown, the target pattern (Fig. 3C) is shaped after several developmental stages for stripe formations.(Unless otherwise mentioned, development *after* evolution is plotted for the fittest individual at 2000th generation.) Next, we examined how the output gene pattern had evolved, by tracing the final output pattern of the ancestors successively. The output pattern after development of the ancestor at each generation is plotted in Fig. 3B, where the color code and spatial axis are identical to those in Fig. 3A, while the horizontal axis represents the generation (evolution time) in Fig. 3B. The similarity between the developmental (Fig. 3A) and evolutionary (Fig. 3B) space-time diagrams are clearly discernible in the figures.

For reference, we have also plotted the developmental course at intermediate (1,300,750,2000) generations in Fig. 3D. With successive generations, novel stripes are acquired, moving the system towards the target pattern.

Development with epochs that correspond to those derived through evolution

Correspondence between developmental and evolutionary space-time diagrams was commonly observed in our simulations (Fig. 3). Additional examples are provided in Fig. 4 and in Supplemental figures. It is remarkable that the pattern formation progressed in a stepwise manner, with respect to both evolution and development. Each stripe emerges not gradually, but discretely at some step in development and in evolution. In other words, the developmental process consists of a few 'epochs' exhibiting rapid changes in the expression pattern, while between two epochs, the pattern is quasi-stationary and changes occur slowly. More interestingly, the correspondence between evolutionary and developmental diagrams is supported by the correspondence of epochs in the two diagrams. This correspondence is valid for a large portion of our simulations. Furthermore, we generally observed good agreement between development and evolution models based on the topology of stripe formation: i.e. how later stripes branched from earlier stripes (see Figs. 3, 4 and Supporting Figure S1).

To quantitatively evaluate the correspondence between evolutionary and developmental spacetime diagrams, we measured the overlap between the diagrams of the output expression levels. The procedure to compute the overlap is shown in Fig. 5A. For both diagrams, we took only the temporal regime in which the pattern formation progressed, i.e., we discarded both the early stages where the output gene was not expressed in all cells (i.e., $x_N(t,l) \sim 0$ for all i), and the final stage after emergence of the stationary pattern, when no additional changes were observed. The distances between the output expression levels for both the diagrams were then averaged over all spacetime pixels, Δ, thus allowing us to compute the differences between the two diagrams. The distribution of Δ from approximately 500 evolution trials for different target patterns is shown in Fig. 5B, with a peak distribution located at approximately 8%.

Note that if the difference between the two diagrams is one stripe over all of the space time pixels, Δ here is evaluated to be 8.2% (Fig. 5B). Hence, the peak value in the distribution is mostly just one stripe difference over all space time. Thus for most examples, the space-time diagrams between developmental and evolutionary processes show remarkable similarity. These results suggest that the correspondence between evolution and development is not an accident, but is a general outcome for most evolution samples. We therefore began an investigation to determine why this evo-devo congruence holds so frequently.

Mechanisms of pattern formations

Note that the evo-devo congruence is achieved by correspondence of epochs between evolution and development. Hence, we first needed to understand how epochs are formed in development. At each epoch, pattern changes occur that generate novel stripe(s) or valley(s). We thus needed to study basic mechanisms for pattern formation in development. Through extensive analysis of approximately 500 number of the developmental processes, we confirmed that the stripe formation process is reduced to only two basic mechanisms in gene expression dynamics with corresponding GRN structures. In fact, these two mechanisms have previously been identified and studied extensively, which are known as feedforward and feedback regulations [15–21].

Feedforward

The classic mechanism for stripe formation, which was analyzed in the segmentation process in Drosophila, is feedforward regulation. This mechanism has been analyzed both theoretically and experimentally [22–24]. In this case, a gene 'reads' the morphogen gradient for spatial information, to establish an 'on/off' response under a given threshold level, so that the gene is expressed on the one side of space, and non-expressed on the other side. Another 'downstream' gene receives positive (or negative) input from this gene, and negative (or positive) input from the morphogen, then responds to create another segmen-

tation in space, if the threshold parameters satisfy a suitable condition. By combining this feedforward regulation, more stripes are formed for the downstream gene. The corresponding GRN does not require feedback regulation, or cell-to-cell interaction by diffusion; only unidirectional, feedforward regulation from morphogen input to downstream genes is required. This feedforward regulation frequently exists in our evolved GRN, and is used to generate at least some stripes.

Feedback oscillation within a boundary

The other mechanism for stripe formation, commonly observed in the present simulations, takes advantage of feedback regulation to produce a temporal oscillation in the expression level. This temporal oscillation at a single-cell level is then fixed into a spatial periodic pattern by the diffusion among cells. A typical core network structure and expression dynamics are shown in Fig. 6A. Here, gene A activates the expression of both itself and gene B, while gene B suppresses the expression of gene A. Since this network is just a typical negative feedback loop, it produces a temporally oscillating expression when the parameter values for the expression dynamics are appropriate. Now, with the diffusion of B under an appropriate boundary condition, this temporal oscillation is fixed into a spatially periodic pattern (see Fig. 6B). Consider a case where the input from the morphogen suppresses the activation of A at the boundary. Then at this boundary, the expression of gene B is also suppressed. Protein B then diffuses from this boundary. Subsequently, the suppression of A is relaxed adjacent to the boundary (Fig. 6B, bottom), so that the protein of gene A is fixed to a higher level, instead of oscillating. This leads to an increase in the expression of B. With the diffusion of protein B, the expression of B is increased at the upper sites, which then suppresses the expression of A, so that the expression level of A is fixed at a lower level. With this process, temporal oscillation of one period is mapped into one spatial stripe. The same fixation process is repeated with the subsequent oscillation at further upper sites, since at the nearest lower site, the expression of gene A is fixed to a lower level. Thus, the temporal oscillation is recursively fixed to a spatially periodic pattern. With this mechanism, the stripe pattern in space is formed and fixed (For detailed theoretical analysis, see Supporting Figures S2, S3). The emergence of a fixed point from a limit cycle is understood as a bifurcation, specifically, a saddle node bifurcation on invariant cycle (SNIC). Indeed, SNIC in a globally coupled dynamical system has been studied as a mechanism for cell differentiation from a stem cell [25].

This mechanism is analogous to the classic Turing pattern in which case the suppression of B to itself is necessary to exclude a spatially homogeneous, temporally oscillating state. Here, the diffusion of the inhibitor gene B works in the same way as the Turing pattern [26], but the mechanism in this study is distinguishable from the standard Turing pattern, since the suppression at a boundary triggers the fixation of pattern, instead of the inhibition of B to itself. The mechanism also resembles a classic wavefront mechanism, in which the temporal oscillation is fixed into a spatial periodic pattern through input from the morphogen gradient and the growth of the system size. In the wavefront mechanism, however, diffusion (or cell-to-cell interaction) is not essential, and external manipulation by the morphogen gradient for all cells leads to fixation forming a stripe from the oscillation. In our case, such external manipulation exists only at the boundary, and further stripe formation progresses spontaneously by the diffusive cell-to-cell interaction.

Evo-devo correspondence by combination of the two mechanisms

All of the potential evolved stripe formation processes in our model could be generated by a single combination out of four possible ways of combining these two developmental mechanisms, sequentially. However, for the feedback mechanism to work, the boundary depending on the morphogen has to be established in advance, to fix the temporal oscillations to spatial stripes. Thus, the feedforward mechanism to read the external morphogen is needed to produce the boundary. Otherwise, no stripe will be formed, so that such networks will not remain in the evolutionary simulation. Hence, we consider only two

combinations: feedforward-feedforward and feedforward-feedback. Indeed, these two cases are the bases for all of the developmental processes evolved in our simulation.

Sequential Feedforward mechanisms

Stripe formations involving the combination of feedforward mechanisms have been extensively studied. In some examples, the developmental processes evolved here are achieved by sequentially combining feedforward processes, where cell-to cell interaction is not needed. Consider a new feedforward mechanism, added at some point downstream from an upstream feedforward circuit. As long as the upstream mechanism is not affected by the downstream mechanism (which is true if there is no feedback from the latter to the former), the stripe formation progresses first by the upstream mechanism, and then, at a later epoch, the stripe is generated by the downstream mechanism. This ordering in the developmental process agrees with the order of evolution, since the downstream mechanism is acquired later in the evolutionary course. Hence, in this simple sequential feedforward mechanism, the evo-devo correspondence is a natural outcome. For the evo-devo congruence to occur over time, the stripe formation has to occur sequentially in developmental time, with some delay, as would occur in evolution. This requires the existence of a slow developmental process, whose origin will be discussed later.

The evolved network illustrated in Fig. 7A consists of a combination of sequential feedforward networks and a downstream feedback network. Through evolution, first the feedforward network via gene 10 and gene 3 (see Fig. 7D) is acquired at around the 10th generation. Then, a domain in the middle space is shaped in development as shown in Figs. 7B and 7E. Later, at the 88th generation, another feedforward network via gene 12 is attached downstream through evolution (Fig. 7F). With this attached network, a domain is shaped in the interior of the earlier domain as seen in Figs. 7F and 7G, right after the earlier domain formation is shaped. The shaping of domains is successfully completed at an early stage of development. This leads to the evo-devo congruence. Later, this modified domain in the middle works as a boundary condition for the subsequent feedback network to be discussed.

Feedback-Oscillation attached downstream of the feedforward network

This combination is indeed necessary for the feedback mechanism to work as already explained. In this case, the stripe formation by the feedback mechanism cannot work without a boundary, and only after the appropriate boundary condition is generated by the feedforward mechanism. On the other hand, the feedforward circuit is first acquired in the earlier stage of evolution to increase fitness, and later the feedback-oscillation is obtained to create further stripes using the former feedforward stripe as a boundary. Hence, we again observe good agreement in the time courses of stripe formation development and evolution, as long as the latter feedback mechanism does not influence the former feedforward mechanism. Here, in the developmental course, boundary formation by the feedforward mechanism has to be completed earlier in development, where the slow developmental process required for the separation of two epochs is necessary for the evo-devo congruence, as will be discussed later.

An example of evo-devo congruence caused by feedback-oscillation downstream of the feedforward mechanism is displayed in Fig. 7A. Corresponding space-time diagrams of evolution and development are presented in Figs. 7B and 7C. Evo-devo congruence is detected, in particular between the third and fourth upper stripes. These two stripes are generated by the oscillation-fixation mechanism generated by the feedback loop (Fig. 7A), attached downstream of gene 3, which is a component of the feedforward network from a maternal morphogen. This feedback module is inhibited by two morphogens and gene 5, so that this oscillation does not start without an input for activation. The only activation input for this feedback module is gene 3, which is expressed only in a domain restricted by the upstream feedforward network. Thus, the oscillation starts after the expression level of the gene 3 is sufficiently high (Fig. 7I), and thus is bounded within the domain, maintaining the expression of gene 3 (Fig. 7H). Following the

mechanism discussed in the next section, a stripe is generated in this domain. This feedback oscillation is regulated by the upstream feedforward network but does not disturb upstream feedforward expression.

Existence of slow variables in development working as bifurcation parameters

So far, evo-devo correspondence in pattern formation and gene-expression ordering can be adequately explained through the combination of feedforward and feedback networks and the corresponding developmental dynamics. For evo-devo congruence in time, however, the developmental process needs to include time spans without significant changes in the expression patterns between two epochs, since evolutionary change requires time spans sufficient in length to allow for the emergence of relevant mutations. This waiting time in evolution has been observed in our simulations (Figs. 3 and 4), and has also been discussed as punctuated equilibrium [27]. Correspondingly, we have observed a long quasi-stationary regime in development. To clarify the mechanism behind the time separation between the slow quasi-stationary regime, and the epoch for faster stripe formation, we first reveal a slow process in developmental dynamics, representing the origin and function of slow change in some expressions.

How slow change in gene expression works as a control parameter

We initially evaluated how slowly varying expression actually works as a control parameter to change a stripe pattern of an output gene. The expression of the output gene is driven by the expression dynamics of input genes and diffusion. In Fig. 8, we showed the change in expressions of such genes, at the site marked in Fig. 8A, which presents the space-time diagram of the expression of the output gene. Fig. 8B shows GRN and the corresponding expression dynamics between the 1st and 2nd crossing presented in Fig. 8A. As shown, the expression of the output gene was switched between on and off, at the time denoted by the crossed red lines, corresponding to epochs. As seen in Fig. 8C and 8D, the input to the expression of the output gene goes beyond or below its threshold at the time marked by the crossed red lines. This change is driven by the on/off switch of gene A, seen in Fig. 8B. Here, the switching in gene A is mainly driven by the slow change in input, denoted by the gene S in Fig. 8B. The slow change in the expression level of gene S plays a role as a parameter cue providing the timing of the epoch. Morphogen concentration acting on cells is fixed as indicated by the black horizontal line in Figs. 8B and 8C. Morphogens initially activate the output gene that provides the first epoch. The morphogen also activated gene S, whose expression level increased at a much slower time scale than the output gene. When it exceeded the threshold for the expression level of gene 1, the expression increased on a faster time scale, and suppression of the output gene then exceeded the morphogen's positive input. The expression of the output gene subsequently decreased, thus generating the second epoch. The expression of gene S also worked as a slow parametric change for the third epoch, which involved a feedback regulation with gene B, as seen in Fig. 8C. Here, the expression of gene B led to suppression of gene A and expression of the output gene, which generated the third epoch. In this way, the slow change in the expression of gene S worked as a control parameter.

As seen in this feedforward mechanism, an expression level at an upstream gene that works as a slow parameter determines the time-table of its downstream genes. In all of the examples that we studied, genes that slowly change their expression level were always present. This slow change is essential to the formation of the quasi-stationary regime.

The origin of slowness in expression

Questions remained regarding the origins of such slow expression dynamics. Following analysis of all examples, we concluded that the origin of slowness could be attributed to the following two mechanisms:

(i) The existence of genes with small rate constants γ_i associated with expression change. The expression dynamics in our model includes a parameter $1/\gamma_i$, representing the time constant for change. Hence if some gene i has a small γ_i value, expression changes slowly. While this itself may appear rather trivial, it should be noted that the rate parameters γ_i's after evolution are distributed by gene i, and some genes have smaller γ_i values. Therefore, the expression levels of genes with small γ_i values function as a slow variable. Indeed, in the example presented in Fig. 8, γ_i for the gene S is 0.063; a full order of magnitude smaller than the others. Through evolution, genes with distinctively small γ_i values appear, even though we initially established nearly uniform γ_i values for all genes.

(ii) Expression levels near the threshold. The expression dynamics here have a threshold θ_i. If the input to the gene is larger (or smaller) than θ_i, it is expressed (or suppressed), respectively. When the input term from other genes to the gene i is close to θ_i, then, the expression level can be balanced at an intermediate value between 0 and 1. Indeed, if the deviation of input from θ_i is smaller than $1/\beta$, the inverse of sensitivity, then the expression level of $x_i(l,t)$ is no longer attracted to 0 or 1. In this case, this stationary state is less stable than those closer to 0 or 1 (see Supporting text S1 for the mathematical explanation using the Jacobian matrix). Hence, the time-scale around this fixed point is longer in duration.

This slow relaxation to the stationary state as a single-cell dynamic is extended, through the entire space, mediated by the diffusion interactions with other cells. With diffusion, the slow expression change of a certain cell can propagate spatially to other sites, to change their expression levels slowly.

A slowly varying expression level works as a bifurcation parameter to produce a developmental epoch

So far, we have discussed the existence of some expression levels that change slowly over time, which may work as a control parameter for changes in the expression dynamics of other genes. In spite of slow gradual changes for these input parameters, however, there appear several epochs in which expression levels show drastic changes. In dynamical-systems theory, indeed, such drastic change in the state variable is known as a bifurcation of attractors against a parameter change, and the developmental epochs are regarded as bifurcations of some expression level.(Here the term bifurcation refers to the change among states in phase space in the dynamical systems theory; it does not necessarily correspond to branching in phylogenic trees.)First, there is a straightforward consequence of on/off (threshold-function) dynamics on expression: When the input to a given gene changes continuously, its output expression level shows a nonlinear, drastic change as the input exceeds the threshold θ_i. In cell biology, this is supported by a Hill coefficient greater than 1.

Consider the example of the network presented in Fig. 9, with a slowly changing expression of Gene S. When the expression level of gene S (slow variable) increases slowly and reaches a certain level, the expression level of gene A increases from ~ 0 to ~ 1. Input changes to gene B may then lead to bifurcation. Here the morphogen (gene M) activates gene S and gene B, while gene S activates gene A, and gene A subsequently inhibits gene B. If the expression level of gene S is smaller than the total activation input to gene B, the dynamics of expressions of gene A and B are given by the flow presented in Fig. 9 (upper left). The nullcline of gene B forms z-like structure in this phase space, which crosses the perpendicular nullcline of gene A, at coordinates near (0,1). As the expression level of gene S increases, the nullcline for the expression of gene A moves horizontally, so that the fixed point at $(x_A, x_B) \sim (1, 0)$ disappears and is replaced by the fixed point at $(x_A, x_B) \sim (0, 1)$, as seen in Fig. 9 (bottom left). Thus, the bifurcation between fixed point attractors occurs with a change in gene expression level of gene S as the bifurcation parameter.

Bifurcation behind Evo-Devo correspondence

During this study, we observed that the developmental process consisted of a quasi-stationary regime and epochs to form new stripes, due to bifurcations resulting from slowly changing expressions as parameters. This is relevant to achieving evo-devo congruence, since the evolutionary process also consists of a quasi-stationary regime prior to the emergence of a relevant mutation capable of increasing fitness within a relatively short time span. Indeed, such mutations change the gene expression dynamics drastically to form a new stripe, which again is regarded as a bifurcation. At a certain generation in the evolution, a mutation occurs to add an inhibition path from gene S to gene A (Fig. 9). This mutation occurs in a discrete manner: Whether a path exists or not, it is not represented as a continuous change in a parameter value. However, we can introduce a continuous strength parameter that changes from 0 to ± 1, and which can be regarded as a bifurcation parameter. Then with this continuous change, an on/off discrete change appears at a certain value of path strength that depends on the threshold of gene A. The phase diagram of gene A and gene B is shown in Fig. 9(right column), where the abscissa represents the expression level of gene A, while the ordinate represents the expression level of gene B. At a lower strength in the path, the nullcline of gene B expression changes so that the former stable fixed$(1, 0)$ point exhibits a saddle-node bifurcation, to move to another fixed point (0,1). Hence, the mutational change in the network leads to a bifurcation. As seen in Fig. 9, this bifurcation through the evolutionary process agrees with that observed during development.

After examining hundreds of numerical evolution simulations, the results were summarized as follows: Development: slow change during expression works as a bifurcation parameter, and bifurcation in the expression dynamics generates a novel state, which gives rise to an epoch. Evolution: search for mutation resulting in relevant change to a new state. Evolution is also regarded as the same bifurcation. In this way, evo-devo correspondence is achieved through bifurcation.

Violation of Evo-Devo correspondence

Although evo-devo correspondence is frequently observed and is discussed as a natural outcome of the combination of network motifs for development, small, but non-negligible portions of the simulation runs exhibited deviation from this evo-devo correspondence. An example of such an exception is presented in Fig. 10A (See also Supporting Figures S4 and S5 for additional examples). In this example, the developmental and evolutionary diagrams differ distinctly, not only in the timing of the formation of the second and third upper stripes, but also in the topology in their branching. During the course of evolution, there is a drastic change in the final pattern, at approximately 1272-1273 generations. Here, only a single mutation occurred in a GRN (addition of a single path). In this example, the feedback oscillation of gene 5 was responsible for the output gene expression, in particular for the second and third stripes, while the expression of gene 6, which lies upstream of gene 5, acted as a boundary for the feedback oscillation, which also contributed to the expression of the output gene. In Fig. 10B, the gene expression dynamics of the selected genes 5 and 6, as well as the output gene, are displayed for generations before and after this mutation, in the left and right rows, respectively. Here, the mutation occurred upstream of gene 6, and reduced the range in which the gene was expressed, accordingly. The expression around sites 60-70 was subsequently suppressed, allowing for the formation of an additional stripe near site 70, while at lower sites (around site 60) the expression level continued to oscillate, forming a stripe much later. Hence the temporal ordering of the formation of the second (near site 80) stripe, while formation of the third (near site 70) stripe is reversed by this mutation. Indeed, before the mutation, the third and fourth stripes were generated together (while the second stripe did not exist), and after this mutation, the second and fourth stripes were generated together, and the third stripe was shaped later. Thus, the ordering and topological branchings of stripes are altered by the mutation, which led to a violation of the evo-devo correspondence.

To summarize, the violation of the correspondence was due to an upstream expression change resulting

from mutation, which caused a change in the boundary condition for the feedback oscillation of the downstream expression gene. We have studied several other examples that showed a violation of evo-devo correspondence, and confirmed that differences in the topology in stripe branchings between development and evolution is caused by mutation upstream of the feedforward mechanism acting as a boundary of the feedback mechanism (See Supplementary information for additional examples).

Discussion

Summary:

The potential relationship between phenotypic dynamics to shape phenotypes and evolution in genotypes has been the focus of the evo-devo field, since genetic assimilation was first proposed by Waddington [28], and has been investigated in RNA evolution [29] and gene expression dynamics [30, 31], as also summarized in recent reviews [32–34]. Still, studies to establish relationships between multicellular pattern formation dynamics and evolutionary processes that shape the pattern remain premature both in theory and experimentally.

Here, we carried out extensive simulations to evolve gene regulatory networks subject to fitness requirements, in order to generate a predefined target pattern for the expression of a given output gene. The main results of the present paper are summarized as follows:

1: Epochs of development as bifurcation:

The developmental course of the expressions of the output gene, after evolution, consisted of a few epochs characterized by rapid temporal change in gene expression and a quasi-stationary regime with slow temporal change between the epochs. The slow quasi-stationary regime is due to expression levels of some genes that vary slowly over time, while the rapid drastic change is due to a bifurcation in the expression dynamics.

2: Punctuated equilibrium in the evolution of morphology as bifurcation:

Likewise, the evolutionary course of expression dynamics consists of a few epochs with a drastic change, and a quasi-stationary regime between the epochs. The drastic change is again represented by a bifurcation, which is caused by mutations in the gene regulation network.

3. Evo-devo congruence through common bifurcations:

In most cases, we observed good correspondence between development and evolution, with regard to spatiotemporal dynamics, from a uniform state to a target pattern. We observed good agreement between development and evolution when evaluating epoch changes from one pattern to another, as well as ordering. Indeed, the same bifurcations occurred for both, and thus the evo-devo congruence was due to the common bifurcation at each epoch.

4. The combination of feedforward and feedback gene regulation networks to support developmental epochs:

The combination of feedforward and feedback modules in gene regulation networks provides successive bifurcations at epochs. The upstream feedforward network converted the external gradient of the maternal factor into an output pattern, while the feedback loop converted the temporal oscillation of gene expression into a spatial stripe, under a given boundary condition provided by the feedforward expression dynamics. The evo-devo correspondence was preserved as long as the upstream feedforward network was maintained.

5. Violation of evo-devo correspondence through modification of upstream feedforward regulation under downstream feedback mechanism:

In rare examples of our simulated runs, we observed violations of evo-devo congruence. These violations were always associated with a structure of the upstream feedforward network and a downstream feedback loop, in which modification of the upstream feedforward network changed the boundary condition of the downstream feedback.

This then raised questions as to why the sequential feedforward network was excluded therein, and whether the violation always involved the feedforward-feedback combination. The feedforward mechanism reads the morphogen gradient of a maternal factor, so that the feedforward-feedforward process transfers spatial information of the maternal gradient sequentially, from upstream to downstream. The flow of spatial information was unidirectional, so that the downstream genes could not generate new stripes on their own. Since each stripe location was defined by the expression of the upstream genes, the downstream genes could not translate their stripe location parallel. For the violation of evo-devo congruence to occur without the loss of fitness, two mutations, one to delete a stripe and one to add a stripe, had to occur at the same time, otherwise, downstream stripe formation would be damaged, and fitness would decrease. As two such simultaneous mutations are less probable, the violation of evo-devo congruence under feedforward-feedforward network rarely occurred. Conversely, in the case of the feedforward-feedback network, the downstream feedback loop maintained the stripe formation mechanism, and the upstream changes affected only the boundary condition. Hence, as a result of a single mutation, the stripe position could be shifted without destroying it. In this instance, only a single mutation was needed, which is why the violation of evo-devo congruence occurred only in association with the feedforward-feedback network rather than through a sequential feedforward network.

Relevance of our results to developmental and evolutionary biology

Now we discuss the relevance of our results to evolution and development of biological patterns, corresponding to the points noted above.

(**1**) Note that the developmental process evolved in our simulation involved slow change in concentrations of some chemical controlling the dynamics. Slow gradual changes in the concentrations of several chemicals are known to play an important role in the developmental process, which may involve some signal molecules, hormones, and morphogens [35]. The developmental process is generally believed to consist of successive stages, each of which involves time spans with slow gradual change, and epochs involving drastic change leading to the next stage. Novel dynamical processes are necessary for this transition [35]. This is consistent with our observations, while our bifurcation scheme provided an interpretation for commonly observed developmental stages. Because processes that generate such drastic changes are not fully understood, it will be relevant to analyze such changes in terms of dynamical systems, in particular, by bifurcation against slow change in some concentration of chemicals.

(**2**) The existence of a quasi-stationary regime and rapid change are often discussed in evolution in terms of punctuated equilibrium [27]. Indeed morphological changes observed through fossil data have suggested these temporal modes throughout the course of evolution. Our results suggest that such temporal modes can be explained as bifurcation. Indeed, research has suggested that novel developmental events are acquired in evolution as a result of bifurcations (i.e., evolution as bifurcation) [36].

Our results imply that the acquisition of morphological novelty in evolution is achieved by bifurcation in developmental dynamics, although this is difficult to confirm from fossil data. Alternatively, by imposing suitable changes in gene expression dynamics that might correspond to evolutionary change, a novel morphological pattern may be achieved. For example, by introducing a hormone and over-expressing a single gene, Freitas et al succeeded in inducing fin distal expansion and fin fold reduction in zebrafish,

which conceivably represented a prototype of vertebrate appendages [37]. The induced epigenetic change leads to a novel gene expression pattern, thereby generating a stripe pattern. This may correspond to bifurcation of a spatial pattern due to genetic change of expression dynamics in our study.

(**3**) In our study, correspondence between evolution and development is achieved through common bifurcations. It is difficult to check this correspondence directly from experimental data since the morphology is not easily traced through an evolutionary course, while the comparison of phylogeny and ontogeny usually involves examination of the morphology only of present organisms that have diverged from common ancestral species(See Fig. 1). Hence, it is not possible to directly confirm our evo-devo correspondence. However, if the morphological novelty is a result of bifurcation, different novel morphologies can diverge from a common ancestral pattern, through different bifurcations. This viewpoint is consistent with von Baer's third law of embryology, which claims that a common basic morphological feature of the group emerges in advance of special features for each species. If we assume that ancestral features are basic for the group, our result suggests that von Baer's third law is due to morphological constraint and bifurcation of developmental processes induced by genetic change.

Currently, a popular topic in the evo-devo field is to examine the existence of phylotypic stages and the validity of the developmental hourglass [8]. Several recent studies have investigated these topics for different species including Drosophila [9], vertebrates [10], plants [12], Caenorhabditis [12] and the soft-shell turtles [14]. As previously mentioned, our study was unable to provide direct evidence to support the developmental hourglass, since it was not intended for species-wide comparison but for a single chain in the phylogeny to unveil the basic mechanism for the evo-devo congruence. Also, all individuals in our model were subject to the same initial conditions, with suppressed expression of genes under the same external morphogen gradient, which could not adequately mimic the conditions that would be observed for real multicellular organisms [38]. Despite these deficiencies, the results of this study may have relevance to species-wide comparison also. Our results suggest that evolutionary branching from common ancestral pattern to generate diverse morphological patterns occurs through bifurcation in dynamical systems from common ancestral pattern. Diversification from the bottleneck in evolution and development can be understood accordingly, which may give a basis for the hourglass model.

(**4**) The importance of feedforward and feedback regulations in development has now gained more extensive recognition. The relevance of the successive combination of feedforward networks has been recognized in long-germ segmentation processes in Drosophila, together with theoretical analyses [22–24]. On the other hand, the relevance of a feedback loop to form temporal oscillations has been understood for several decades [39–43]. In vertebrates, Pourquié discovered that somite genesis is achieved by mapping this temporal oscillation to a spatial stripe formation, where a wavefront model is applicable [44]. Our mechanism to fix the temporal oscillation to the spatial pattern is similar to the wavefront model, with some differences. In the wavefront model, a combination of the morphogen gradient, size growth, and oscillatory dynamics forms the stripe pattern, while, in our case, a combination of cell-to-cell interaction with diffusion and oscillation leads to stripe formation under the boundary conditions provided by upstream feedforward gene regulation. This distinction will be experimentally verifiable by determining whether the cell-to-cell interaction is essential to stripe formation.

Here we also demonstrated the importance of the feedforward-feedback combination, to read external morphogen information leading to robust stripe formation in a bounded domain, where the boundary condition to determine the domain is supported by the upstream feedforward network. Complex gene regulatory networks in the present organisms often include a combination of feedforward-feedback networks [35], although their functional roles have not necessarily been fully defined. It will be important to elucidate the role of the feedforward network as a boundary-maker and the role of the feedback loop in robust patterning, as suggested here.

(**5**) Experimental confirmation of the violation of evo-devo congruence through modification of the upstream feedforward network, with a conserved downstream feedback loop, is expected to be difficult, considering limitations in available evolutionary data. Therefore, we propose to examine whether morphological novelty arises as a result of modification of upstream feedforward regulation under feedback regulation. While direct examination of our feedforward-feedback hypothesis from the data is difficult, it is possible to evaluate the hypothesis by externally destroying the upstream feedforward network while retaining the feedback loop.

Future Issues

The present study is an initial step towards resolving the larger issue of evo-devo correspondence. Even within the present model, a number of issues remain to be clarified, as follows:

(i) Even though we have confirmed that our result is independent of the details in the model, such as the cell number, gene number, model parameters, and the form of the external morphogen profile, further study is necessary to confirm the universal applicability of our results.

(ii) In the gene expression dynamics after the evolution, we found that there always exists a slowly varying gene expression level that works as a control parameter. Thus far, we have not uncovered the conditions responsible for the emergence of this slower mode, which controls other expressions that are relevant to fitness. By modifying coupling with this slower mode, the output behavior that it controls is more readily altered, so that evolution can be facilitated. Therefore, the emergence of slowly varying expression(s) may be evolutionary advantageous. It is important to investigate the generality of the emergence of this slow variable.

(iii)We have not observed the classic Turing mechanism [26] in the developmental process by evolved networks. Under the influence of a morphogen gradient, it may be natural to use the maternal information effectively with respect to evolution. It is then an open question whether without the external information (but by imposing the boundary condition instead), the Turing-pattern mechanism can evolve dominantly.

(iv)How do evolutionary reachability of the target and complexity in the developmental process depend on the predefined target pattern? It may be expected that as the target pattern is more complex, it takes more time to evolve GRN to produce such patterns, and development involves more epochs, but is there a way to quantitatively characterize such complexity?

(v) We have explained evolution-development congruence in terms of the correspondence of epochs, but it is not clear whether quantitative congruence exists beyond this level. For example, does the time span for the quasi-stationary regime between two epochs correlate between development and evolution? In other words, if the evolutionary search time to generate a relevant mutation for the next epoch is longer, then, is the quasi-stationary regime before the epoch also longer in development? Our preliminary results suggest that this correlation exists for cases where small Δ values are observed, while further analysis is required to clarify the conditions and mechanisms for such congruence.

(vi)Extension of our model for higher spatial dimensions, introduction of size (cell number) growth through development, and inclusion of recombination in a genetic algorithm will be important in future studies. Furthermore, it is important to note that real morphogenesis in multi-cellular organisms is far more complex than these models, and is not necessarily governed only by the reaction-diffusion mechanism. Cell rearrangement under mechanical stress could also play an important role, and inclusion of development mechanisms will be important. Still, we also note that previous research has indicated that

macroscopically represented, stress-induced pattern formation can also be represented by equations of the reaction-diffusion type [45]. Hence, the present conclusions on evo-devo congruence through bifurcations may be applicable beyond development based on a reaction-diffusion scheme.

(vii)Last but not least, the implications of our single-chain-phylogeny study on species-wide comparison have to be explored. For example, by adding population division and speciation process with imposing different target pattern to the model, species-wide extension will be available. That future study will be important not only for the validation of our results, but also for further understanding of evo-devo relationship in species-wide comparison.

Concluding remark

In contrast to recent advances in experiments aimed towards analyzing the evo-devo relationship at a quantitative level, theoretical studies based on dynamical systems and statistical physics are still in their infancy. While we acknowledge that our current model may be oversimplified, we hope that the present work can act as a springboard to launch future cooperative efforts in the field of evo-devo between theories and experiments.

Methods

Gene Regulation Network(GRN) model for pattern formation

A cell's state is represented by the expression levels of k genes/proteins, $x_i(l,t)$, involving the protein expression levels of the i-th gene in the l-th cell at time t, representing N genes ($i = 1, ., N$) and $M(= 96)$ cells, aligned in a one-dimensional space. A protein expressed from each gene either activates, inhibits, or does not influence, the expression of other genes, in addition to itself. For simplicity, we assumed that the change in the i-th protein expression level is given by the equation:

$$\frac{dx_i(l,t)}{dt} = \gamma_i(F(i,l,t)) - x_i(l,t)) + D_i\frac{d^2x_i(l,t)}{dl^2} \tag{1}$$

with

$$F(i,l,t) = f(\sum_j J_{i,j}x_j(l,t) - \theta_i) \tag{2}$$

where the term $-x_i(l,t)$ in (1) provides a measure of the degradation of the i-th protein with γ_i as its rate [15, 16, 46, 47]. The expression level is scaled so that the maximum level is unity. The function $f(x)$ is similar to a step function, where the function approaches 1 as x is increased to a positive side, and approaches 0 as $x_i(l,t)$ is decreased to a negative side: In other words, if the term $\sum_j J_{i,j}x_j(l,t)$ is sufficiently larger than the threshold θ_i, then $F(i,l,t) \sim 1$, which indicates that the gene is fully expressed, and if it is smaller than the θ_i, then $F(i,l,t) \sim 0$, which indicates that the gene expression is suppressed. Here, we chose, $f(x) = 1/(1 + e^{-\beta x})$, where β, which was set to 40, denoting the sensitivity of the expression at the threshold. Roughly speaking, it is proportional to the Hill coefficient.

The gene regulation network was introduced to our model based on work reported in earlier studies. In Fig. 2, each node of the network represents a gene, and the edge of the network represents the interaction between genes, given by $N\times N$ matrix $J_{i,j}$: where J_{ij} is 1, j if it activates the expression of the gene i, -1 if it suppresses the expression, and 0 if there is no connection. All cells have an identical regulatory network, with the same parameter values, which are determined by genes.

Finally, the last term in Eq. (1) shows the diffusion of a protein, between neighboring cells, with D_i as the diffusion constant. For the majority of the simulations described here, we set $M = 96$, and $N = 16$, while preliminary simulations adopting larger values for these did not alter the conclusion in the paper.

Initial/boundary condition

As an initial condition, the expression levels of all genes were set to 0. Furthermore, external morphogens, which are denoted as the proteins 0 and 1, are supplied externally. Fixed linear morphogens are induced from both sides for cellular use, so that $x_0(l,t) = x_0(l) = (M-l)/M$ and $x_1(l,t) = x_1(l) = l/M$. We also evaluated a case involving a gradient with an exponential dependence in space, as $\mathrm{Cexp}(-l/\xi)$, but this condition did not alter the conclusions presented in this study. Discrete Neumann boundary conditions were adopted at both ends for this study, i.e., $x(1) = x(2)$ and $x(M) = x(M-1)$.

Definition of fitness

To study the evolution of morphogenesis, we imposed a fitness condition to generate a given specific target pattern, for the expression of a given output gene. By setting a target pattern as $T(l)$, the fitness f_i was defined as the sum of the distance between this target pattern and output gene expression at each cell, as:

$$f_i = \sum_l 1 - |T(l) - x_{output(l)})| \tag{3}$$

where l is a cellular index. From the equation, the smaller the distance, the higher the fitness. Here the output gene pattern was defined after a given transient time, which was chosen to be large enough to reach a stationary pattern. For each genotype (i.e., GRN and a set of parameter values), the fitness was thus computed, after simulating each set of pattern dynamics.

For this analysis, we chose 100 individuals with different genotypes. Among these individuals, those who had higher fitness values were preferred to be selected for the next generation. Selection of the individual i with a fitness value of f_i was defined by

$$p_i = \frac{e^{f_i}}{\sum_k e^{f_k}} \tag{4}$$

The denominator summation of index k is aimed for all individuals in the population.

To generate the offspring, each genotype was slightly modified. A path in GRN was added, eliminated, or its sign was flipped with the probability $1/N^2$. Also, the parameter values α, D, θ were modified by adding a random number from a Gaussian distribution $\eta(x) = \frac{1}{\sqrt{2\pi\sigma^2}} exp(-\frac{x^2}{2\sigma^2})$, while restricting these values to the set [0,1]. We set $\sigma = 0.01$.

Acknowledgments

The authors would like to thank Tetsuhiro Hatakeyama, Shuji Ishihara, and Naoki Irie for useful discussions. This work was partially supported by a Grant-in-Aid for Scientific Research (No. 21120004) on Innovative Areas "Neural creativity for communication" (No. 4103) and the Platform for Dynamic Approaches to Living Systems from MEXT, Japan.

References

1. von Baer KE (1828) Ueber entwicklungsgeschichte der thiere. Beobachtung und Reflexion. Königsberg: Bornträger.

2. Darwin C (1859) The origin of species. London: John Murray

3. Müller F (1869) Facts and arguments for Darwin. London: John Murray.

4. Hall BK (2000) Balfour, Garstang and de Beer: the first century of evolutionary embryology. Am Zool 40: 718–728.

5. Gould SJ (1977) Ontogeny and phylogeny. Boston: Harvard University Press.

6. Hall BK (1999) Evolutionary developmental biology. Berlin: Springer.

7. Richardson MK, Keuck G (2002) Haeckel's abc of evolution and development. Biol Rev 77: 495–528.

8. Hazkani-Covo E, Wool D, Graur D (2005) In search of the vertebrate phylotypic stage: a molecular examination of the developmental hourglass model and von Baer's third law. J Exp Zool B 304: 150-8.

9. Kalinka AT, Varga KM, Gerrard DT, Preibisch S, Corcoran DL, et al. (2010) Gene expression divergence recapitulates the developmental hourglass model. Nature 468: 811-4.

10. Irie N, Kuratani S (2011) Comparative transcriptome analysis reveals vertebrate phylotypic period during organogenesis. Nat Commun 2: 248.

11. Domazet-Lošo T, Tautz D (2010) A phylogenetically based transcriptome age index mirrors ontogenetic divergence patterns. Nature 468: 815-8.

12. Quint M, Drost HG, Gabel A, Ullrich KK, Bönn M, et al. (2012) A transcriptomic hourglass in plant embryogenesis. Nature 490: 98-101.

13. Levin M, Hashimshony T, Wagner F, Yanai I (2012) Developmental milestones punctuate gene expression in the *Caenorhabditis* embryo. Dev Cell 22: 1101–1108.

14. Wang Z, Pascual-Anaya J, Zadissa A, Li W, Niimura Y, et al. (2013) The draft genomes of soft-shell turtle and green sea turtle yield insights into the development and evolution of the turtle-specific body plan. Nat Genet 45: 701-6.

15. Salazar-Ciudad I, Newman SA, Solé RV (2001) Phenotypic and dynamical transitions in model genetic networks. i. emergence of patterns and genotype-phenotype relationships. Evol Dev 3: 84-94.

16. Salazar-Ciudad I, Solé RV, Newman SA (2001) Phenotypic and dynamical transitions in model genetic networks. ii. application to the evolution of segmentation mechanisms. Evol Dev 3: 95-103.

17. François P, Hakim V, Siggia ED (2007) Deriving structure from evolution: metazoan segmentation. Mol Syst Biol 3: 154.

18. Fujimoto K, Ishihara S, Kaneko K (2008) Network evolution of body plans. PLoS One 3: e2772.

19. Cotterell, James and Sharpe, James (2010) An atlas of gene regulatory networks reveals multiple three-gene mechanisms for interpreting morphogen gradients. Mol Syst Biol 6: 425.

20. ten Tusscher KH, Hogeweg P (2011) Evolution of networks for body plan patterning; interplay of modularity, robustness and evolvability. PLoS Comput Biol 7: e1002208.

21. Alon U (2007) Introduction to Systems Biology: And the Design Principles of Biological Networks, volume 10. Boca Raton, Florida: CRC press.

22. von Dassow G, Meir E, Munro EM, Odell GM (2000) The segment polarity network is a robust developmental module. Nature 406: 188–192.

23. Jaeger J, Surkova S, Blagov M, Janssens H, Kosman D, et al. (2004) Dynamic control of positional information in the early drosophila embryo. Nature 430: 368–371.

24. Ishihara S, Fujimoto K, Shibata T (2005) Cross talking of network motifs in gene regulation that generates temporal pulses and spatial stripes. Genes Cells 10: 1025–1038.

25. Goto Y, Kaneko K (2013) Minimal model for stem-cell differentiation. Phys Rev E 88: 032718.

26. Turing AM (1952) The chemical basis of morphogenesis. Philos Trans R Soc London Ser B 237: 37

27. Eldredge N, Gould SJ (1972) Punctuated equilibria: an alternative to phyletic gradualism. Models Paleobiol 82: 115.

28. Waddington C (1957) The strategy of the genes: a discussion of some aspecs of theoretical biology. London: Allen and Unwin.

29. Ancel LW, Fontana W (2000) Plasticity, evolvability, and modularity in RNA. J Exp Zool B 288: 242–283.

30. Ciliberti S, Martin OC, Wagner A (2007) Robustness can evolve gradually in complex regulatory gene networks with varying topology. PLoS Comput Biol 3: e15.

31. Kaneko K (2007) Evolution of robustness to noise and mutation in gene expression dynamics. PLoS One 2: e434.

32. Wagner A (2005) Robustness and evolvability in living systems. Princeton: Princeton University Press.

33. Kaneko K (2006) Life: an introduction to complex systems biology, volume 171. Berlin: Springer.

34. Soyer OS (2012) Evolutionary systems biology, volume 751. Berlin: Springer.

35. Carroll SB, Grenier J, Weatherbee S (2009) From DNA to diversity: molecular genetics and the evolution of animal design. Hoboken, New Jersey: Wiley.

36. François P, Siggia ED (2012) Phenotypic models of evolution and development: geometry as destiny. Curr Opin Genet Dev 22: 627-33.

37. Freitas R, Gómez-Marín C, Wilson JM, Casares F, Gómez-Skarmeta JL (2012) *Hoxd13* contribution to the evolution of vertebrate appendages. Dev Cell 23: 1219–1229.

38. Sander K, Schmidt-Ott U (2004) Evo-devo aspects of classical and molecular data in a historical perspective. J Exp Zool B 302: 69–91.

39. Goodwin BC (1963) Temporal organization in cells. a dynamic theory of cellular control processes. New York: Academic Press.

40. Chance B, Pye K, Higgins J (1967) Waveform generation by enzymatic oscillators. Spectrum, IEEE 4: 79–86.

41. Cooke J, Zeeman E (1976) A clock and wavefront model for control of the number of repeated structures during animal morphogenesis. J Theor Biol 58: 455–476.

42. Horikawa K, Ishimatsu K, Yoshimoto E, Kondo S, Takeda H (2006) Noise-resistant and synchronized oscillation of the segmentation clock. Nature 441: 719–723.

43. Masamizu Y, Ohtsuka T, Takashima Y, Nagahara H, Takenaka Y, et al. (2006) Real-time imaging of the somite segmentation clock: revelation of unstable oscillators in the individual presomitic mesoderm cells. Proc Nat Acad Sci USA 103: 1313–1318.

44. Pourquié O (2003) The segmentation clock: converting embryonic time into spatial pattern. Science 301: 328–330.

45. Murray JD (2002) Mathematical biology, volume 2. Berlin: Springer.

46. Glass L, Kauffman SA (1973) The logical analysis of continuous, non-linear biochemical control networks. J Theor Biol 39: 103–129.

47. Mjolsness E, Sharp DH, Reinitz J (1991) A connectionist model of development. J Theor Biol 152: 429–453.

Figure Legends

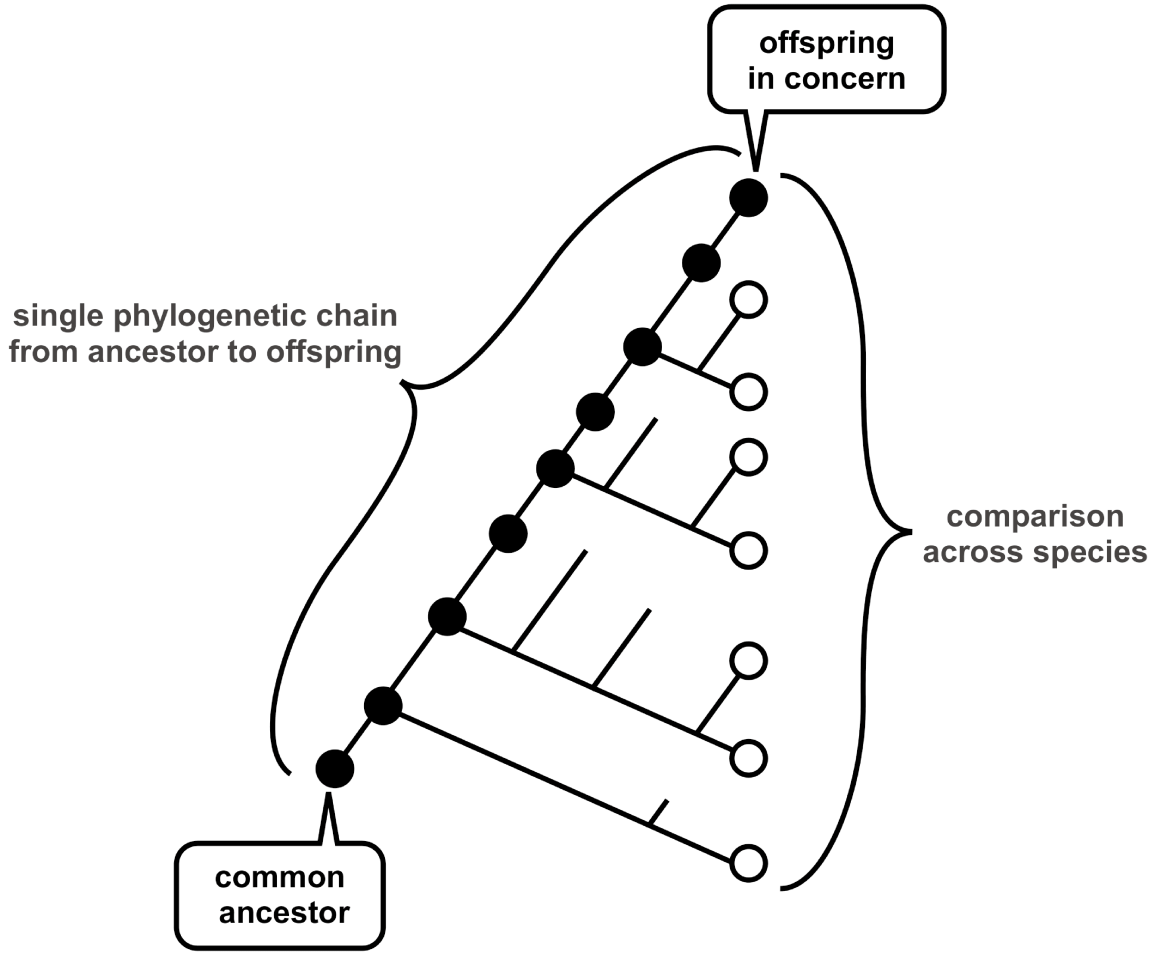

Figure 1. Schematic representation of single-chain-phylogeny and comparison across species in phylogenic tree

Schematic representation of the comparisons along single-chain phylogeny and across species. In the phylogenic tree shown here, the currently existing species represented by the right-end circles, are diverted from a common ancestor. Branching from a common ancestor leads to establishment of some new species, while some are terminated by extinction. The comparison of developmental processes across species is made over the existing species. On the other hand, a single phylogenic chain, which we focused in this study, is given as the line from the common ancestor to the offspring in concern. From the species in concern, ancestors are uniquely traced back. The comparison of developmental processes along this chain is possible at least in theory or simulations, which provides fundamental information on possible relationship between development and evolution.

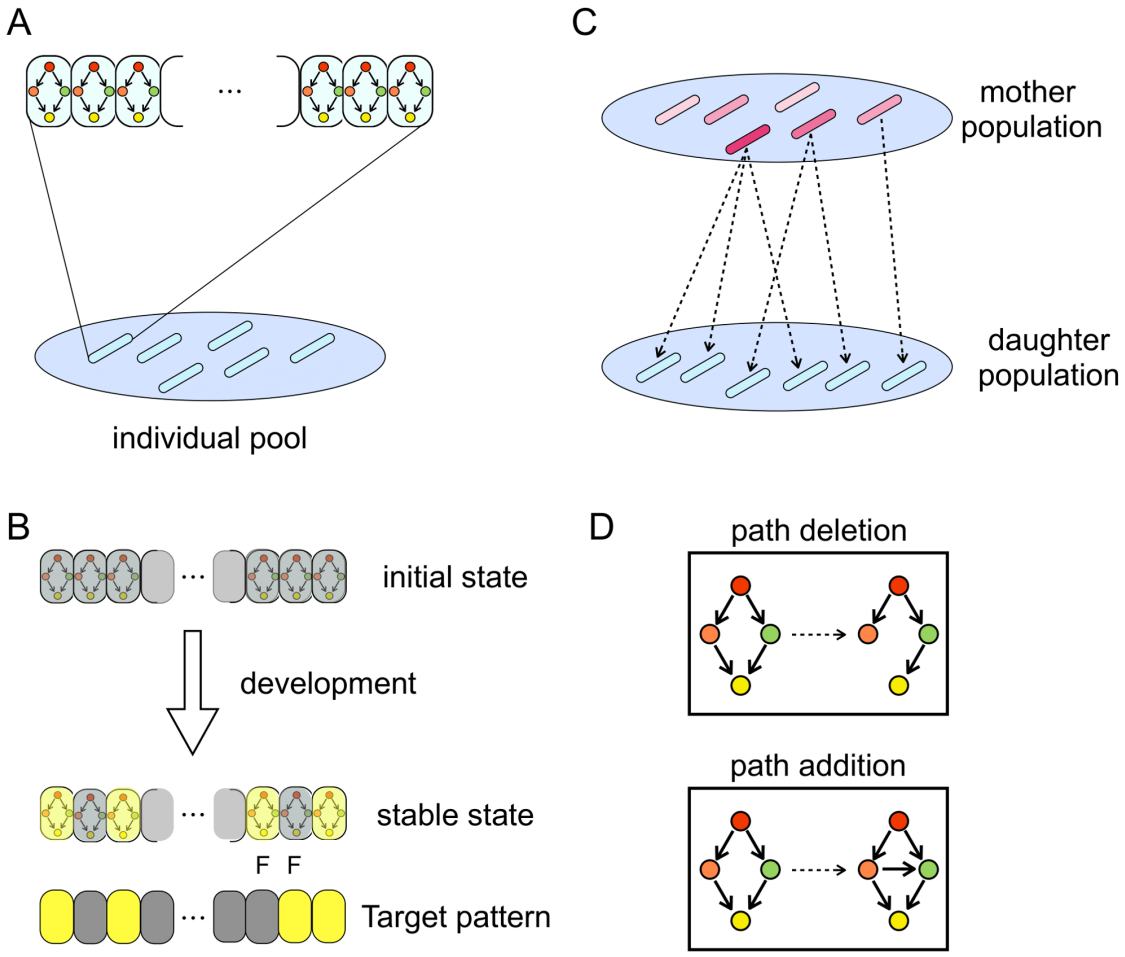

Figure 2. Schematic representation of simulation procedure.
(**A**): There are 100 individuals in a pool for each generation. Each individual consists of 96 uniform cells, which share a common GRN, while the GRN differs slightly between individuals.
(**B**): Each individual develops from the same initial state in which genes are not expressed(i.e., with $x \sim 0$) except for genes receiving the maternal gradient. Over time, individuals develop into stable states. Colors of cells indicate the expression level of the output genes; yellow is high, gray is low. After reaching a stable state, the expression pattern of the output gene was compared with the predefined target pattern. The fitness level was then elevated as the stable expression of the output gene approached the target pattern (see Methods for detail).
(**C**): After the fitness of every individual was calculated, the population for the next generation was created. Each individual was selected as a mother with a probability proportional to its fitness. In the figure, the degree of red color indicates the fitness.
(**D**): The GRN of a daughter is slightly different from the mother's, with a given mutation rate. The mutation involves deletion or addition of paths in the mother's GRN, and a change in characteristic parameters in expression dynamics and the diffusion constant (see Methods for details).

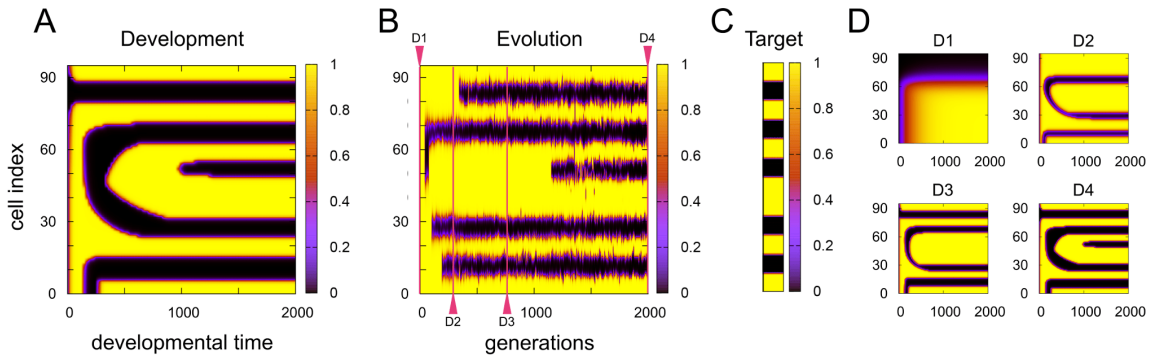

Figure 3. An example of space-time diagram of evolution and development.
(**A**): The expression level of the output gene is shown with developmental time as the horizontal axis and cell index (spatial position) as the vertical axis. The expression level of the output gene of the corresponding cell at a given time is color coded, (side bar) with black indicating the lowest and yellow indicating the highest expression levels. Development consists of a few epochs with rapid changes in the pattern, separated by quasi-stationary regimes with little change in the pattern, until the target pattern is shaped by development.
(**B**): The spacetime diagram of the evolutionary course, corresponding to (**A**). The expression level of the final output gene (at time=2000) is shown with evolutionary generation as the horizontal axis and cell index (spatial position) as the vertical axis. This figure shows how the pattern is acquired through evolution. At each generation, the final pattern of the direct ancestor of the next generation is shown. The evolution of the developed output pattern consists of quasi-static regimes sandwiched by epochs with rapid change resulting from mutation, until the target pattern is evolved.
(**C**): The predefined target pattern adopted in the present simulation.
(**D**): Space-time diagram of the developmental process for several generations in (**B**). Each figure shows the development of the ancestral expression pattern at each generation, 0(D1), 300(D2), 750(D3), and 2000(D4). For reference, these generations are each marked by a red triangle at the top or bottom in (**B**).

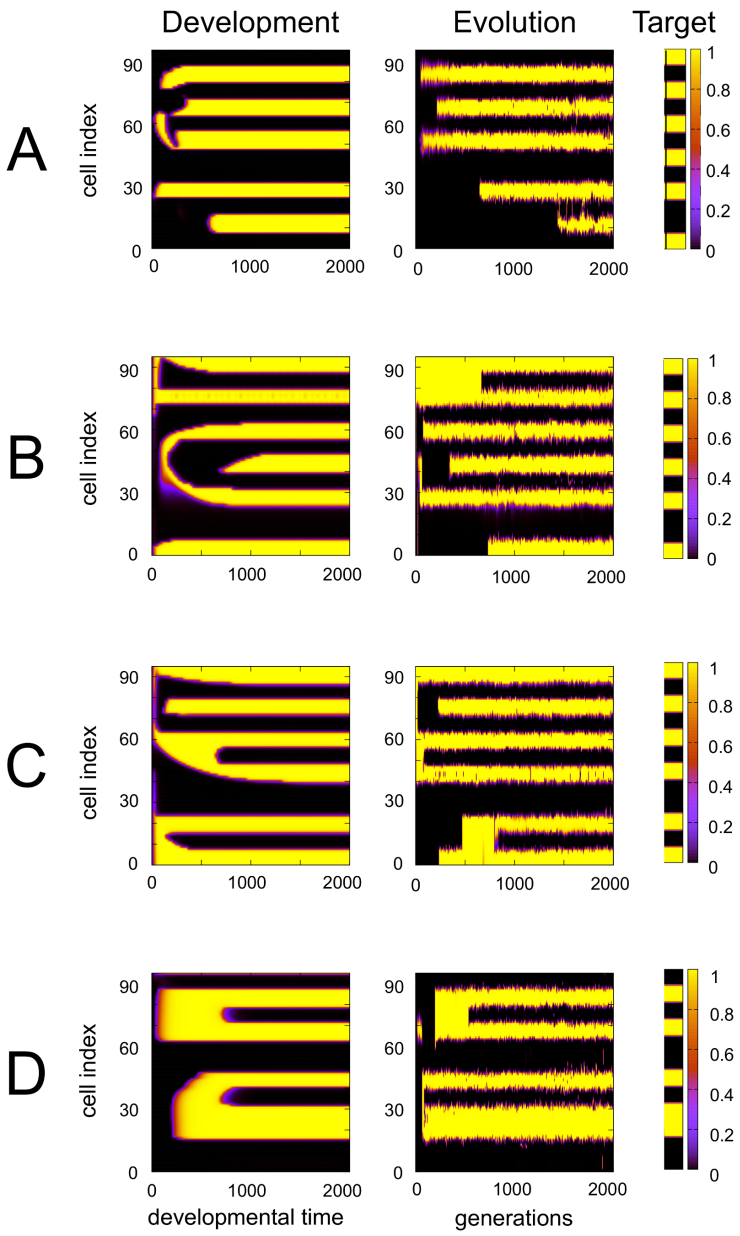

Figure 4. Four additional examples of evo-devo congruence.
(**A**)-(**D**): Each row shows space-time diagrams of evolution and development, in the same way as Fig. 3, although the target patterns are different. See supplemental information for additional examples.

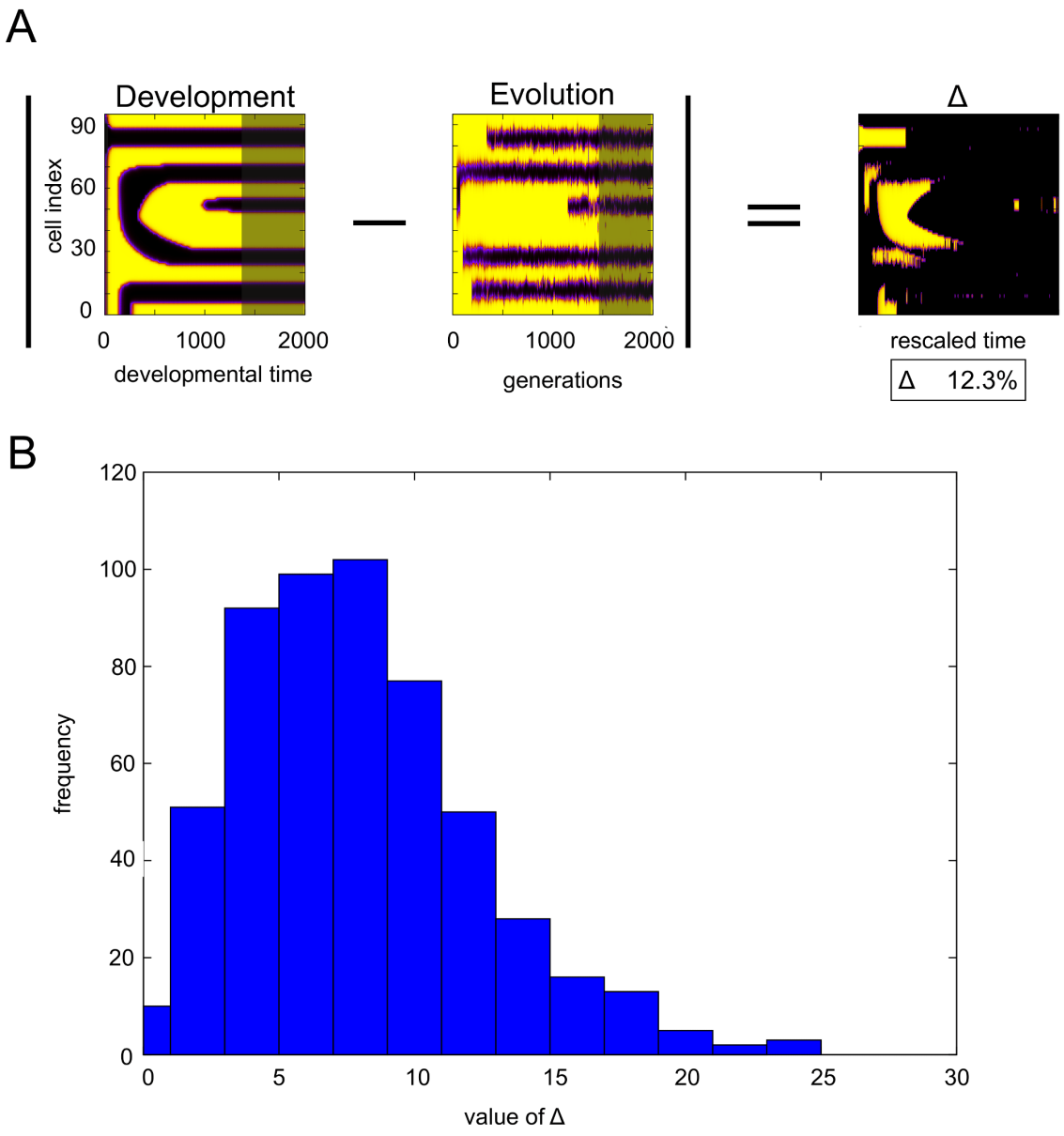

Figure 5. Quantitative analysis of the degree of evo-devo congruence.
(**A**): Schematic diagram illustrating quantitative analysis of the similarity between evolution and development. The differences between development and evolution were computed by subtracting expression levels at each pixel. By taking the absolute value of difference, and averaging the space-time pixels, the average difference was computed . To avoid over-estimating similarity, the region before the emergence of the first stripe and after the final pattern was ignored for both development and evolution. For example, the gray-masked region of the development and evolution figures does not include data for the calculation. If one stripe is completely shifted in time, is approximately 8%.
(**B**): Histogram of the distribution of the Δ values. The abscissa is the Δ value computed via the procedure described in (**A**). The ordinate is the frequency of touch Δ values determined by bin size 2 . Distribution was obtained from 500 runs with different target patterns.

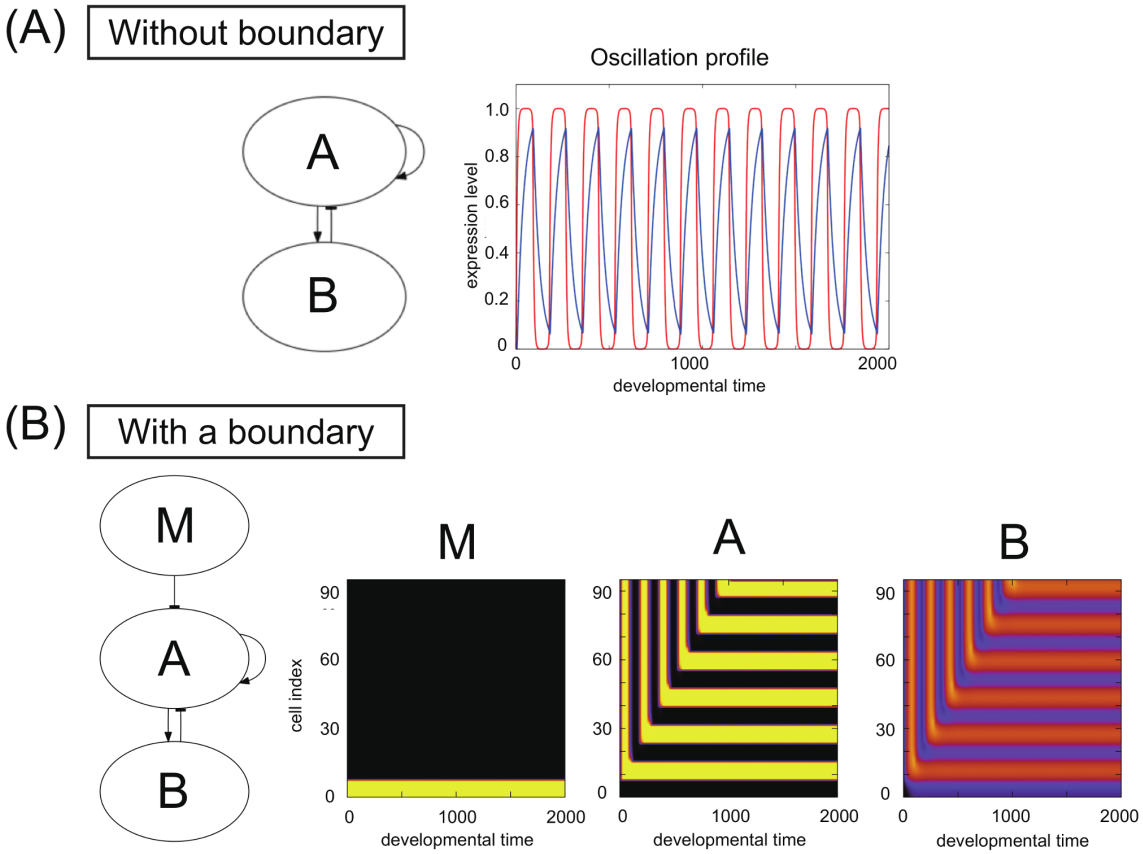

Figure 6. Feedback oscillation and its fixation.
(**A**)**Without boundary:** Minimal network for oscillatory expression with the time series of the expression for a specific cell. Gene A activates the expression of gene B and itself, and gene B suppresses A. In the plotted time series, developmental time is plotted as the abscissa, and the expression levels of A (red) and B (blue) are plotted as the ordinate.
(**B**)**With a boundary:** The input from gene M, which was influenced by the maternal factor, was included in the oscillatory network. The space-time diagram of genes M, A, and B illustrate how oscillatory expressions of gene A and gene B were fixed to form stripes. Gene M was expressed near the boundary.

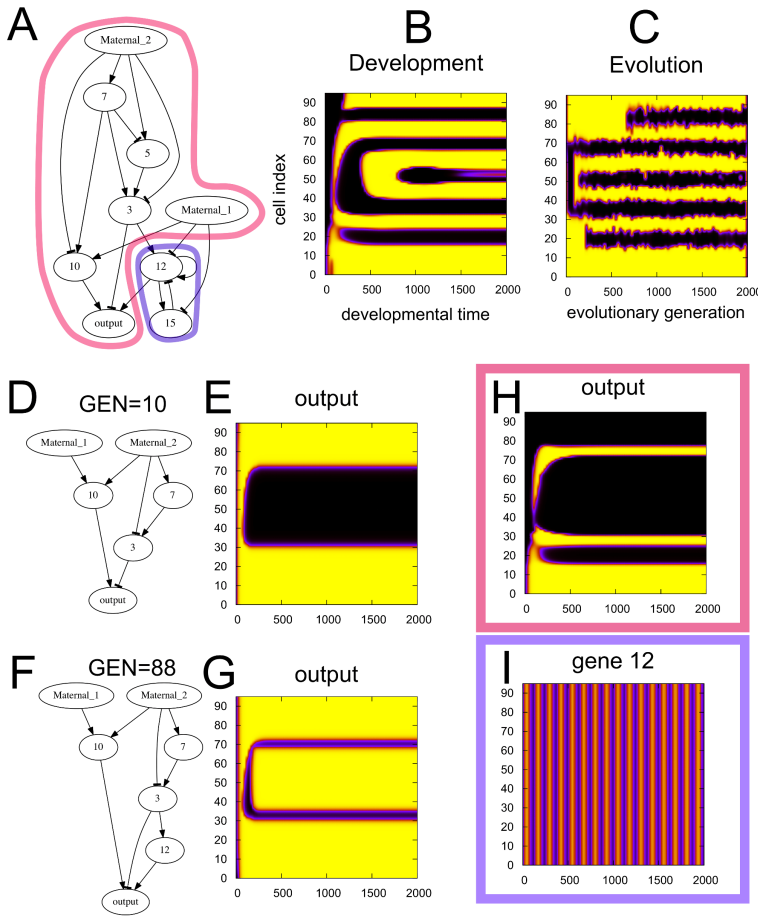

Figure 7. Example of evo-devo congruence with network structures
(**A**): An example of a core part of the GRN at the 2000th generation, evolved to achieve the target pattern. From the maternal factors, the feedforward networks is surrounded by magenta, while the network module for feedback oscillation, consisting of genes 12 and 15, is surrounded by blue. Here, genes and paths that are not essential to the output pattern formation were eliminated.
(**B,C**):Space-time diagrams of the output gene expression for development (**B**) and evolution (**C**) or the GRN are displayed together to show the degree of similarity between them. The vertical axis denotes the space (cell index), and the horizontal axis denotes either evolutionary generation (evolution) or developmental time (development). For this example, the Δ value is 8.0%.
(**D**): An example of the core part of the GRN at the 10th generation (i.e., very early generation) and the corresponding space-time expression diagrams of the output.
(**E**). Feedforward structure of the GRN is evolved at this early stage of evolution. The vertical axis of the phase diagram denotes the space (cell index), and the horizontal axis denotes developmental time. This expression is observed at a very early stage of development in (**B**), at approximately the 10th generation.
(**F**): The network structure at the 88th generation. Through evolution, feedforward structures are sequentially acquired in the downstream region of the core part of the GRN.
(**G**): Developmental space-time diagram of the expression of the output gene for the network **F**. This expression profile provides the top and bottom stripes in (**B**).
(**H**): Developmental space-time diagram of the output expression of the 2000th generation where the feedback oscillation module is eliminated. Without feedback, only part of (**B**) is generated.
(**I**):Developmental space-time diagram of the expression of gene 12, one of the feedback modules in (**A**), which produces a spatially homogeneous and temporally periodic oscillation if constant activation is applied by gene 3. The combination of this feedback oscillation and the boundary condition provided by gene 12 shown here produces the three internal stripes in (**B**).

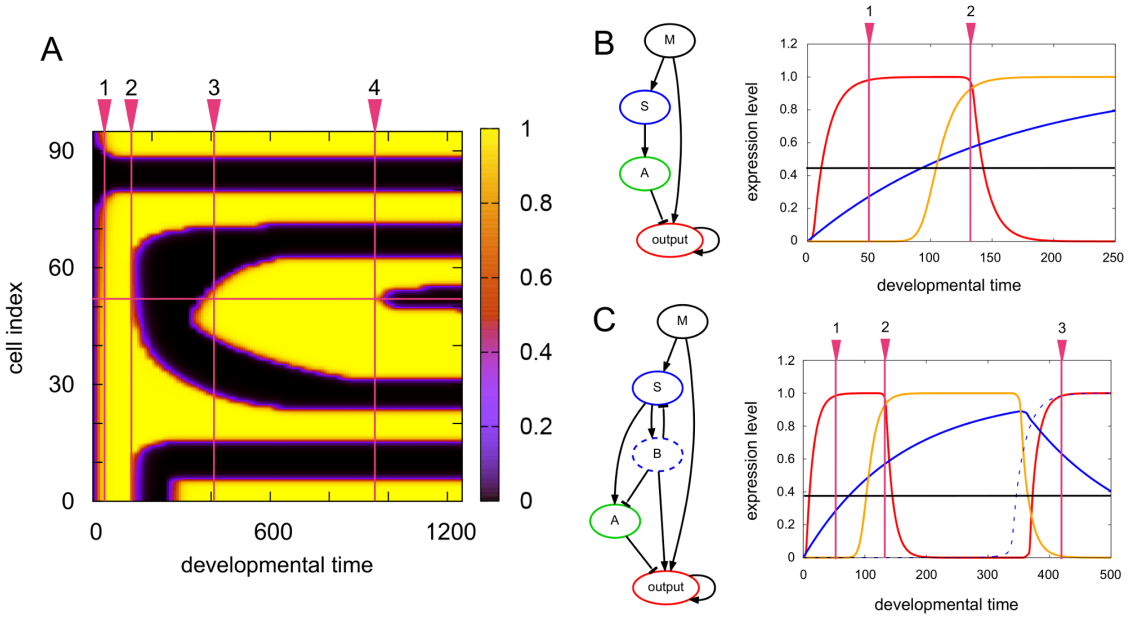

Figure 8. An example of development dynamics with several epochs for a single cell. (**A**): Developmental space-time diagram of the output expression level, plotted in the same way as data in Fig. 3 except for developmental scale is 0 to 1250, which aims to clearly distinguish epochs. There are four epochs associated with one cell, marked by crossing of the red lines.
(**B**): The core network that functions to switch the output expression from the first to second epoch. Expression dynamics of gene S (blue), gene A (green), and the output gene (red) during the time span between the 1st and 2nd epochs are displayed together. Following activation from a maternal factor, the output gene expression is initially high. Over time, the expression of gene S increases slowly, exceeding the threshold of gene A, which then suppresses the expression of the output gene, reaching the 2nd epoch. During this process, bifurcation of the gene expression dynamics occurs. This generates a developmental epoch, as a consequence of change in the slow variable (i.e., the expression level of S).
(**C**): The core network that functions to switch the output expression, from the first to third epoch. Some regulations from gene B are added to the GRN displayed in (**B**). The expression threshold of gene B is higher than that of gene A. After reaching the second epoch, gene S maintains a slow increase and its expression exceeds the threshold of gene B. Regulations from gene B occur, which create another bifurcation similar to the one described in (**B**), and the cell state reaches the third epoch.

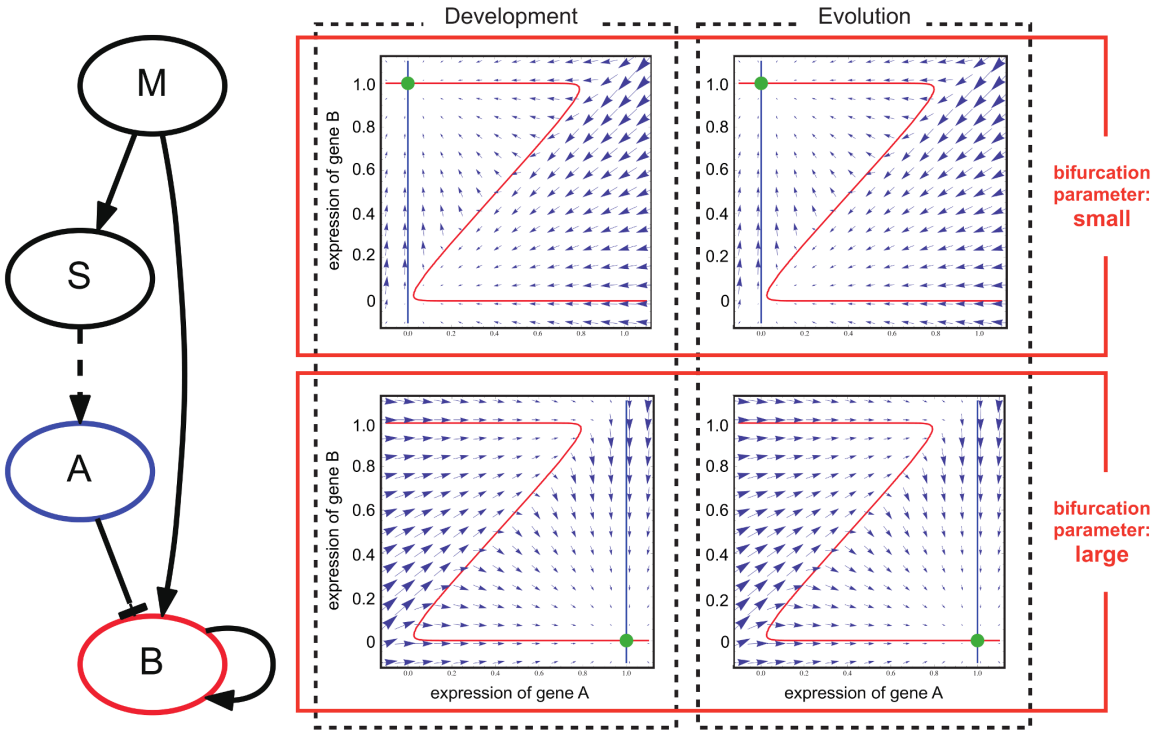

Figure 9. Evolution and development as bifurcation.
The network structure where the expression level of gene S changes slowly (left). Phase space diagrams plotting the expression levels of gene A (horizontal access) and gene B (vertical access). The blue line represents the nullcline of gene A, and the red line represents the nullcline of gene B (right). The green circle denotes the final stable cell state from the initial conditions in each of the diagrams.
Development(left column): Expression level of the slow variable works as a bifurcation parameter. While the expression of gene S is lower than the threshold of gene A, the stable fixed point can be found at approximately ($x_A \sim 0$,$x_B \sim 1$)(upper left). As development progresses, the expression level of gene S increases, and after the expression of gene 1 exceeds the threshold of gene A, the nullcline of gene A shifts slightly to the right, indicating a higher value (lower left). Gene A inhibits the expression of gene B, so that the fixed point is changed to ($x_A \sim 1$,$x_B \sim 0$).
Evolution(right column): Phase diagram representing the expression levels of gene A (horizontal axis) and gene B (vertical axis). The blue line represents the nullcline of gene A and the red line represents the nullcline of gene B. The activation strength from gene A to gene B is regarded as a continuous value here. If the activation strength is low, the expression level of gene 1 is low, so that the stable fixed point is observed at approximately ($x_A \sim 0, x_B \sim 1$)(upper right). When the strength is sufficiently large, the expression level of gene 1 assumes a higher value so that the fixed point is observed at approximately ($x_A \sim 1, x_B \sim 1$)(lower right). Note that by comparing these two columns, a strong correspondence is observed in bifurcation between evolution and development.

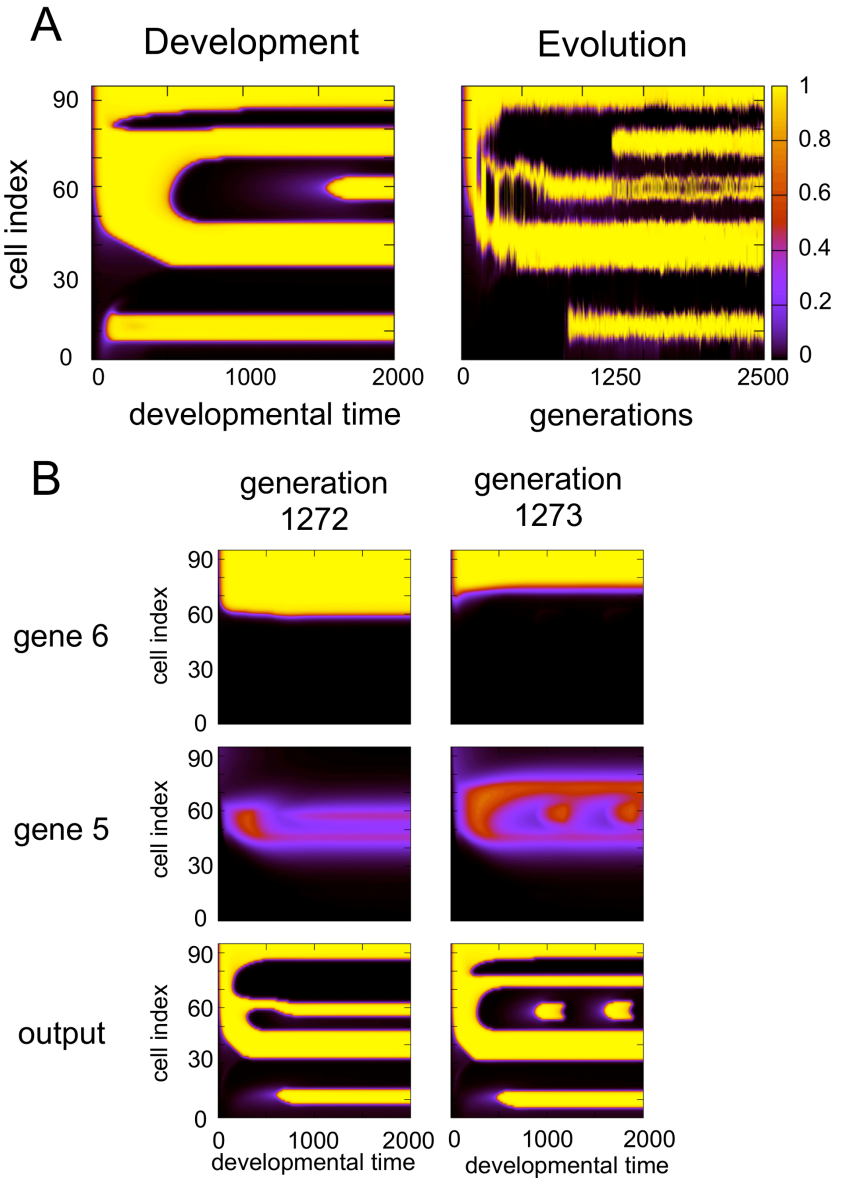

Figure 10. Violation of evo-devo congruence.
(**A**): **Evolution:** The expression level of the final output gene (at time=2000) is shown with the generation (horizontal axis) and cell index (vertical axis). The color scale is presented as a side bar, as in Fig. 3B. According to the figure, the second upper stripe is acquired at the most recent stage of evolution, and the first, third and fourth upper stripes branch from the same root, so that the second stripe emerges from the first upper valley.
Development: Space-time diagram of the expression with developmental time (horizontal axis) and cell index (vertical axis). The third upper stripe emerges at the most recent stage of development. Unlike evolution, the first, second and fourth upper stripes branch from the same root, and the third stripe emerges from the second upper valley. Here, evo-devo congruence is topologically violated.
(**B**): Developmental diagrams plotted for generations 1272 and 1273. These genes show drastic change in their expression between the two generations. Gene 6 provides a feedforward regulation to the output, and inhibits the expression of gene 5, which is a component of the feedback loop to generate oscillatory expression. A mutation, which adds a path to gene 6, occurs between the two generations, which inhibits the expression of gene 6. Through this mutation, the expression of gene 6 is suppressed, thus shrinking the resulting stripe, and producing an additional stripe for gene 5. With this change, the ordering of the expression of the output gene is altered.

Supporting Information

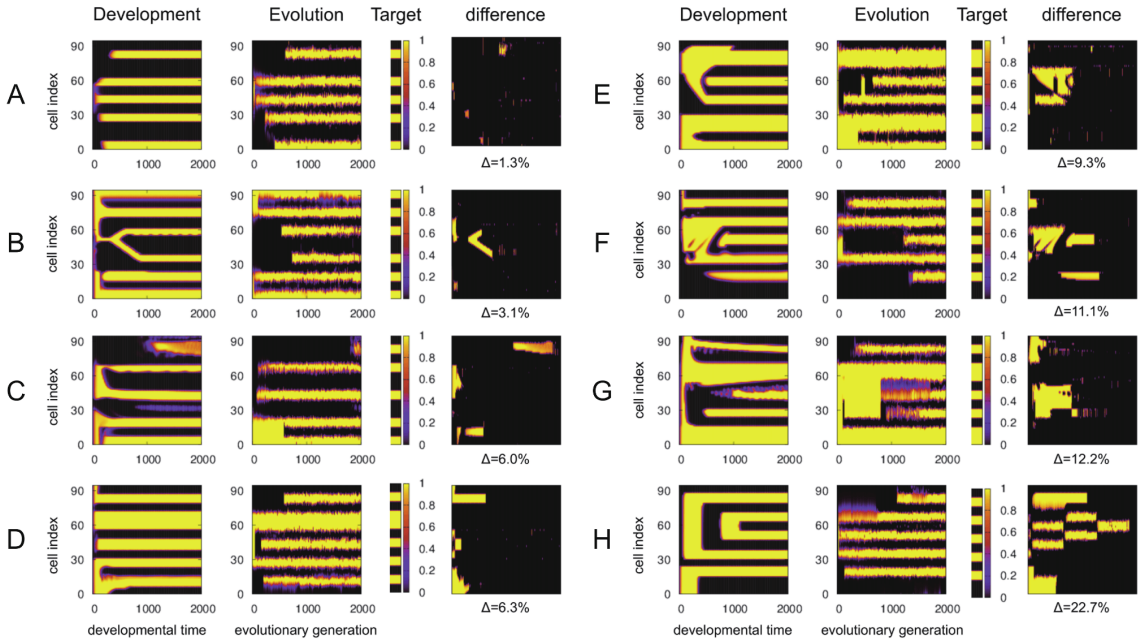

Figure S1. Space-time diagrams of evolution, development and differences between the two.
(**A**)-(**H**) Eight additional space-time comparisons between evolution and development. Each consists of a space-time diagram of development, evolution, preset target pattern and difference between evolution and development. Space-time diagrams of evolution and development and their target pattern are plotted in the same way as in Figs. 3 and 4. Calculated values of the difference Δ are shown below the diagram. For A-D, the evolution and development corresponded well, while a clear violation was observed for H.

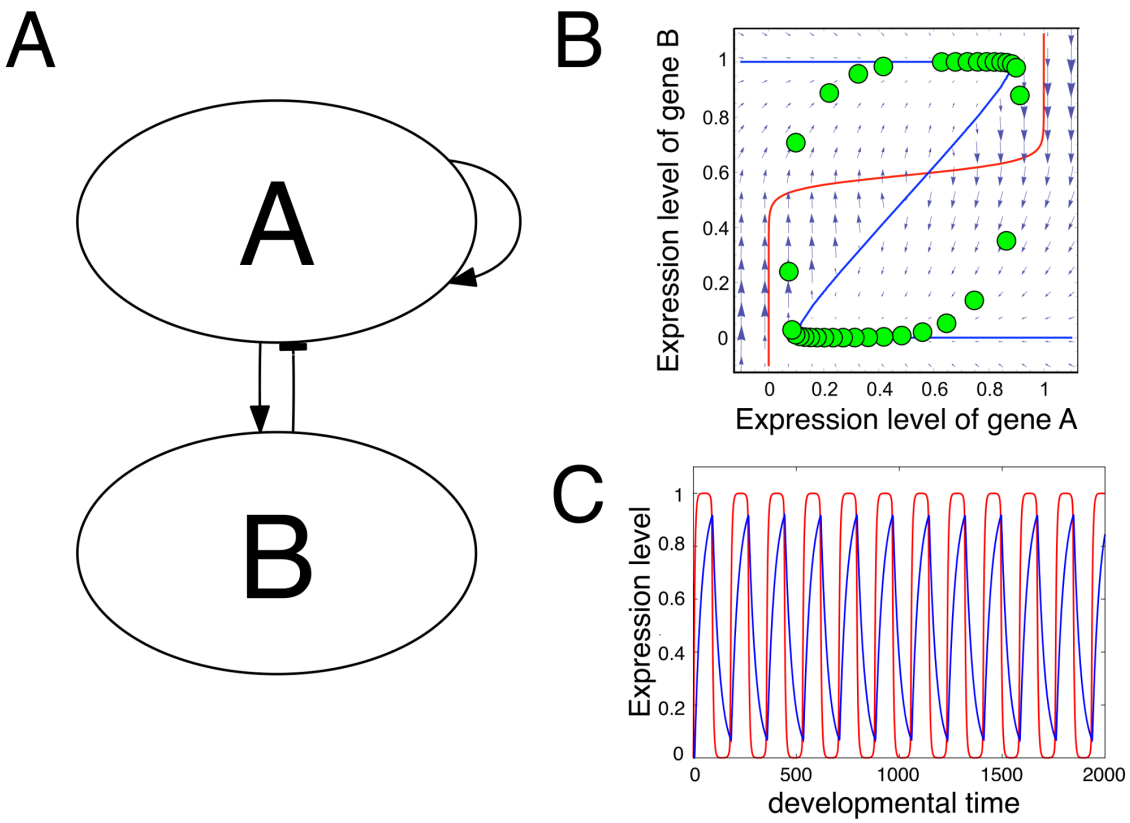

Figure S2 Detailed analysis on feedback oscillation.
(**A**): network structure for data presented in Fig. 6.
(**B**): Phase diagram of the expression dynamics. Two nullclines of gene expression cross at a single, unstable fixed point, and the cell state will oscillate on a limited cycle. Green circles represent the cell state at time step intervals of 5, within a single cycle. The distance between two nullclines is shortest at the upper right and lower left corners so that cell state changes are slower at these corners.
(**C**): Time profile of the feedback oscillation for a specific cell. The abscissa represents developmental time and the ordinate is expression level. Gene A is plotted as a red line, while gene B plotted as a Blue line.

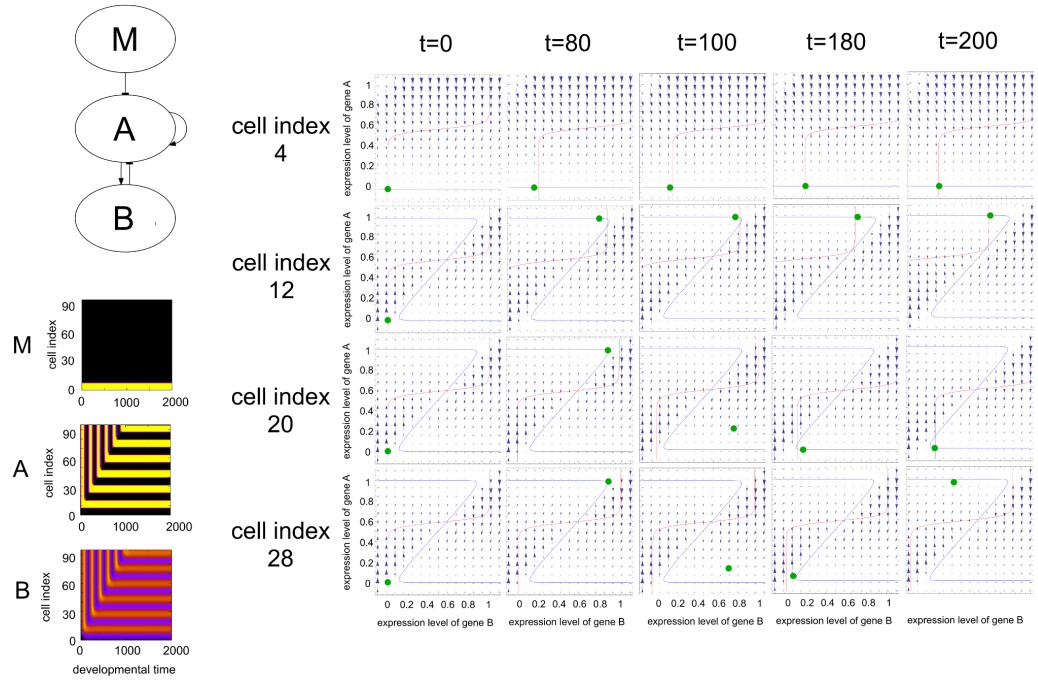

Figure S3 Temporal change of flow in the phase space over cells.
The oscillation fixation mechanism is revealed through comparison of flow temporal changes in the phase space over cells. The central cells of the first two stripes (cell indices 12 and 28) and valleys (cell indices 4 and 20).

(1)**t=0**:
Both gene A and gene B assume a null value, and gene B is inhibited by gene M within the first 8 cells. With these two initial conditions, flow in the phase space where cell index = 4 is different from other cells. At a stable fixed point therein, both the expressions of gene A and gene B are low (i.e., a low-low state). This fixed point is the root of the first valley.
(2)**t=80**:
As development begins, expression of non-inhibited cells begin to oscillate and move towards a state where both expressions of gene A and gene B are high (i.e., a high-high state), while cells of the first valley maintain the slow-low state. Thus, protein A diffuses from the first stripe to the first valley. Due to the incoming diffusion of protein expression of gene A, at cell index 4, the nullcline of gene A slides to the right, so that the expression of gene A assumes a higher value. Correspondingly, at cell index 8, the nullcline of gene A slides to the left, and crosses the nullcline of gene B to create a fixed point.
(3)**t=100**:
The expression of cell index 4 is constrained to the newly formed high-high fixed point. However, the expressions of cells at index 20 and 28 continued to oscillate.
(4)**t=180**:
Through the oscillation, cell index 20 approaches a low-low state for the second time, and at this time, protein B at the first stripe diffuses to the second valley. Thus, nullclines slide in the cells at indices 12 and 20 to the left and right, respectively. The nullcline of gene B then crosses, at a low-low state, in the cell at index 20.
(5)**t=200**:
The expression level at cell index 28 continued to oscillate while that at cell index 20 was

constrained at the newly formed low-low state fixed point, similar to cell index 12 at t=80. Protein B subsequently diffused from the cell index 28 to the second valley, which resulted in the emergence of the second stripe. In this way stripes were shaped from the oscillation.

Text S1 Mathematical analysis of the slow variable

Here we considered the relaxation time around a fixed point. For simplicity we considered the case with $\gamma_i = 1$, to demonstrate that the relaxation time is longer even without the change in γ. The stability of the fixed point was given by eigenvalues of the Jacobian matrix W_{ij} where the diagonal component W_{ii} is given by -1 and the off-diagonal component W_{ij} is given by $J_{ij}\beta exp(-\beta X_i)/(1 + exp(-\beta X_i))^2$ where $X_i = \sum_j J_{ij}(x_j - \theta_j)$. If x_j's are close to 0 or 1, their deviation from θ_j is sufficiently larger than the detection threshold $1/\beta$, the off-diagonal elements are close to zero, and the eigenvalues are given by -1 (or -γ_i if it is not 1). When x_j's takes on intermediate values closer to θ_i, the off-diagonal elements assume larger values, and the eigenvalues are shifted from -1, either upwards or downwards. Hence, some exponents approach zero. As long as the real components of the eigenvalues are negative, the fixed point remains stable, but the stability is weaker, with the exponent closer to zero. This results in an increase in the timescale of the relaxation, given by the inverse of the real component of the eigenvalue. With this mechanism, the slowly changing variable is generated even without small γ_i.

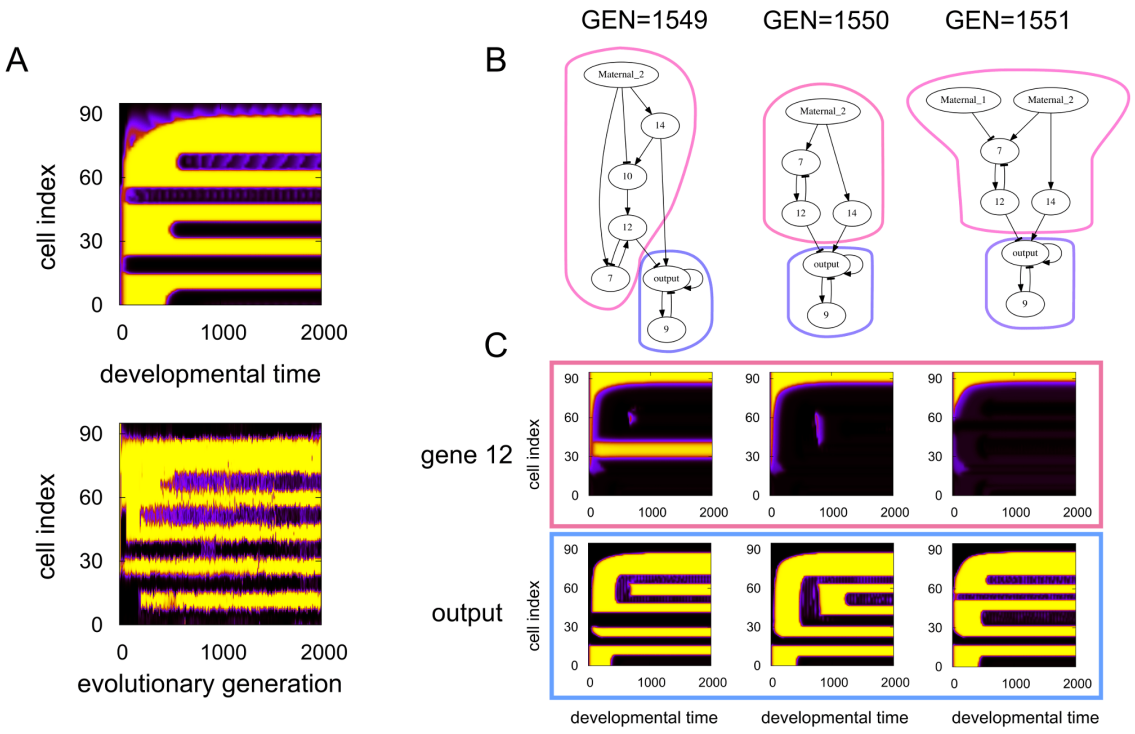

Figure S4 Network analysis of the extra example of the violation of evo-devo congruence 1.
In development, the third and fourth upper stripes stem from the some root, while in evolution the top three stems originate from the same root. This branching change occurs during generation 1549 where the second and third branches are clearly stabilized. In this case, unlike the former examples, topological changes in branching occur sequentially during three generations. A time-space diagram of the output and gene 7 are presented in Fig. B. Gene 7 exhibits two stripes from generation 1549, which are driven by a feedforward mechanism. Due to the boundary effect of gene 7, the upper three stripes are generated in the output gene.

Then, during generation 1550, part of the feedforward mechanism upstream of gene 7 is deactivated, which enhances the region expressed by the feedback oscillation mechanism. As a result, the upper four stripes that emerge share the same oscillation mechanism.

At generation 1551, mutation occurs upstream of gene 7, so that the morphogen comes to inhibit the remaining feedforward mechanism. Before the mutation, gene 7 exhibits weak temporal expression in cell sites 30-85. After the mutation, this temporal expression is inhibited so that the expression region is restricted to cell sites 60-85. Due to this change, the third and the fourth upper stripes emerge faster than the first and second stripes, while the third stripe, generated in advance of the first two, provided a boundary to generate the second stripe.

To summarize, the upper 4 stripes were generated by the feedback oscillation mechanism, but the change in the boundary condition due to mutation in the upstream feedforward mechanism introduced the branching combination.

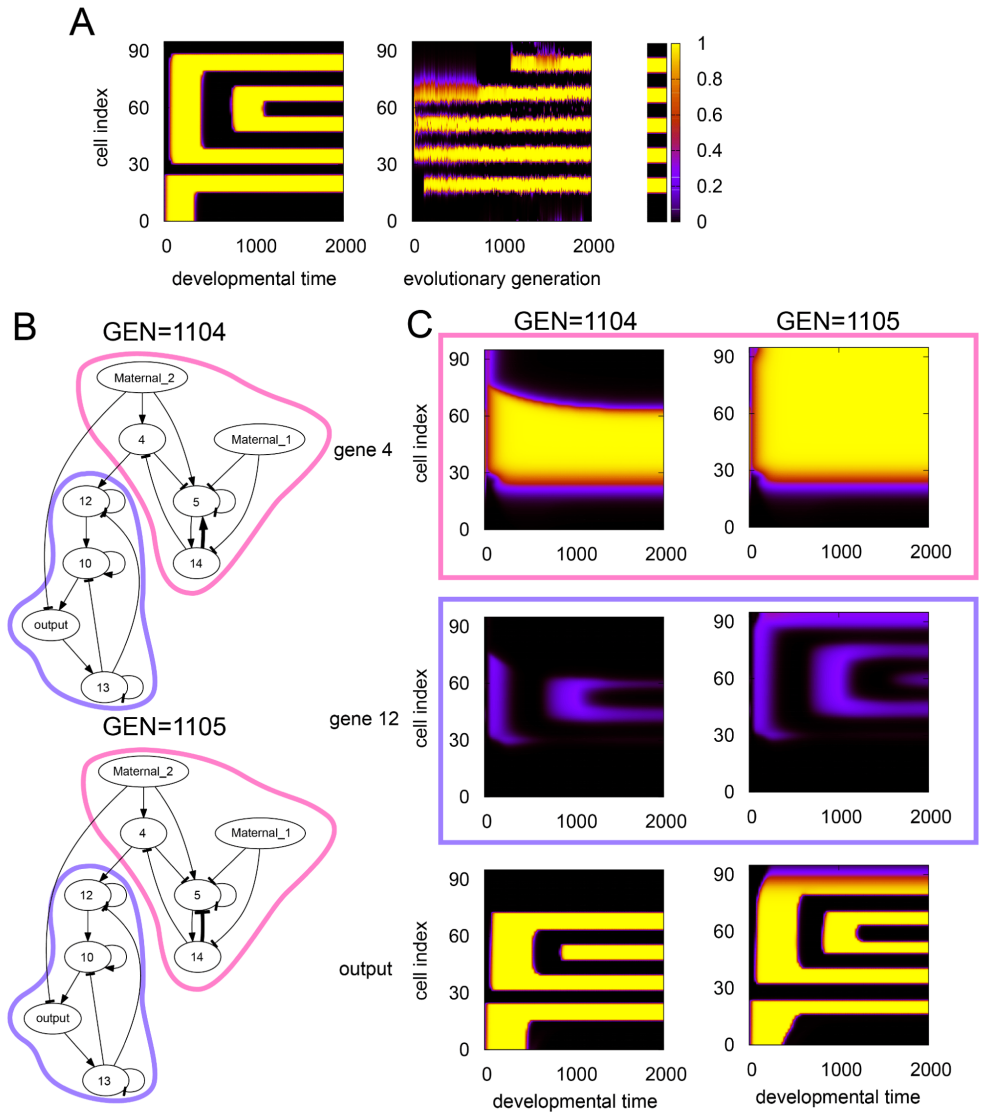

Figure S5 Network analysis of an additional example of the violation of evo-devo congruence.
In evolution, the three central stripes are acquired nearly simultaneously, and two additional stripes are subsequently acquired independently. However, in development, at the final evolved generation, the 1st and 4th stripes were generated from the same root at the same time, and subsequently the 2nd and 3rd stripes were generated from a common root. These two branchings follow the oscillation-fixation mechanism. Only the bottom stripe is generated independently. The developmental order of stripe formation was acquired, between generations 1104 and 1105.

Genes that exhibited relevant change are displayed in Fig. B. The expression of an upstream gene (green in the GRN figure below) and the downstream gene (red in the GRN figure) are plotted at the upper and lower columns, respectively. In this example, the feedforward

mechanism worked only temporally, as shown in the transient expressed before time step = 100 (Fig. C). This temporal expression region also corresponded to the region of feedback oscillation. Due to the mutation, the spatial domain of the transient expression was extended upward. Violation of evo-devo congruence was therefore induced by this expansion of the transient expression region.